

# Molière theory of multiple Coulomb scattering with ionization and the transport mechanism of the multiple scattering process

Takao Nakatsuka

*Okayama Shoka University, Okayama 700-8601, Japan*

Jun Nishimura

*The Institute of Space and Astronautical Science, JAXA, Yoshinodai, Sagami-hara 229-8510, Japan*

(Received 21 January 2008; published 27 August 2008)

The Molière theory of multiple Coulomb scattering is improved to take account of ionization loss by applying a differential formulation of the theory. Distributions for the deflection angle  $\vec{\theta}$ , as well as for any linear combination between  $\vec{\theta}$  and the lateral displacement  $\vec{r}$ , under the ionization process are derived by a series expansion with the same universal functions  $f^{(n)}(\vartheta)$  of Molière, except that the values for both the expansion parameter  $B$  and the scale angle  $\theta_M$  are corrected from those under the fixed-energy process. We find that Goudsmit-Saunderson angular distribution with ionization is also expressed by the same characteristic parameters  $B$  and  $\theta_M$  derived above by the Molière theory. The transport mechanism of Molière process of multiple Coulomb scattering and the stochastic property of Molière series expansion are also investigated and discussed.

DOI: [10.1103/PhysRevE.78.021136](https://doi.org/10.1103/PhysRevE.78.021136)

PACS number(s): 05.60.Cd, 96.50.sd, 96.50.sh, 11.80.La

## I. INTRODUCTION

An accurate theory of multiple Coulomb scattering improves the precision of our designs and analyses of experiments relating to fast charged particles. It also gives reliable results in computer simulations for those experiments. There exists a long history of theoretical works to predict and clarify the stochastic properties of the process. We first constructed the theory by focusing on the central Gaussian profile of angular distribution [1]. Investigations from this point of view, called the Gaussian approximation [2], have been well accomplished by the Fermi-Yang diffusion equation to give the simultaneous distributions among directions of motion, lateral displacements, and longitudinal detours of charged particles [3–5], even under the ionization process [6–8]. Later, the theory was made more precise and applicable to a wider angular range, taking account of large-angle scatterings in the single-scattering cross section [9–15]. The Goudsmit-Saunderson theory and the Molière-Bethe theory are the representative ones in this scheme, and have been widely used. The former accurately derived the angular distribution based on the addition theorem for spherical harmonics [9,10,15]. The latter proposed a diffusion equation assuming the small angle approximation [2] and derived the angular distribution considering energy loss [11–13] as well as the distribution for an arbitrary linear combination between the deflection angle and the lateral displacement under the fixed-energy condition [16].

Although the Molière-Bethe theory is less accurate at large angles than the Goudsmit-Saunderson theory due to the small angle approximation, it still has many benefits in typical and practical applications. The angular distribution is described in a simple series expansion with universal functions, and the angular distribution is easily obtained with accuracy from the first few terms of the series. The distribution is characterized by only two parameters, the expansion parameter  $B$  and the scale angle  $\theta_M$  for deflection angle [17]. As the

theory is described in a standard diffusion equation, we can understand the related problems totally by comparing the results with those from the Fermi-Yang equation [3,4,8] and shower theories [3,18,19], and so on. So it has been widely used in the design and analysis of experiments relating to charged particles and in the trace of passages of charged particles in Monte Carlo simulations [20–22]. However, despite its excellent mathematical foundations, almost no theoretical improvements have been made out of the Molière-Bethe formulation.

Kamata and one of the present authors proposed another formulation of the Molière theory when investigating the effects of single scattering on their cascade shower theory [18,19]. They described the diffusion equation in a simple ordinary differential equation in the frequency space of Fourier transforms. It was just a thorough extension of the Fermi-Yang formulation, but with the addition of a logarithmic term corresponding to the large-angle scattering to the Fermi equation [3,4]. Using their formulation, correction terms by single scattering to solutions under the Gaussian approximation were evaluated on other problems, such as longitudinal-detour problems [5] and shower theories [18,19]. Two constants,  $\Omega$  and  $K$  specific to materials, were introduced in their formulation, appearing in coefficients of the diffusion equation. As all the scattering properties of the materials, including mixed or compound materials, were contained in these constants, it became far easier and simpler to obtain the Molière angular distribution for charged particles traversing through any material. Their formulation is equivalent to the Molière-Bethe formulation, as the both formulations neglect Fourier components of the second higher orders and more against finite constants and logarithmic terms, and gives the Molière angular distribution of simple series easily by using a transport formula indicated in Appendix B. As they remained the fundamental equation differential with the traversed thickness even after they applied Hankel transforms to the angular variable, we could call their

formulation the differential formulation of the Molière theory [23].

We have found other superior aspects of the differential formulation of the Molière theory to be very useful in practical applications. We obtained more accurate angular distributions, as well as distributions for arbitrary linear combinations between the deflection angle and the lateral displacement, taking account of ionization loss, for relativistic charged particles of  $\beta \simeq 1$ , by only introducing the contraction factor  $\nu$  for the traversed thickness. For charged particles of moderate energies, as wide ranges of  $\beta$  as Molière and Bethe applied their theories [11–13],  $\nu$  is evaluated by a numerical integration. And we found Goudsmit-Saunderson angular distributions with ionization are expressed explicitly with the above two parameters  $B$  and  $\theta_M$  derived in Molière theory through the differential formulation. The scattering constants  $\Omega$  and  $K$  for pure materials, as well as those for mixed or compound materials, are also revised by using the values in the Table of Atomic and Nuclear Properties of Materials in *The Review of Particle Physics* [24].

The shape of Molière distribution is determined by the expansion parameter  $B$ , sometimes called the shape parameter [25]. As is well known, the first multiple scattering term of the Molière series is corrected by the second single-scattering term by the magnitude of  $B^{-1}$ .  $B$  showed a monotonous increase with traversed thickness under the fixed-energy process. However,  $B$  under the ionization process increases more slowly and begins to decrease at the last stage of the traverse. This fact is hard to understand, so we investigate and clarify the transport mechanism of the multiple scattering process.

## II. MOLIÈRE ANGULAR DISTRIBUTIONS WITH IONIZATION FOR RELATIVISTIC CHARGED PARTICLES

We first derive the angular distribution of singly charged particles penetrating through uniform materials with relativistic energies by the differential formulation of the Molière theory [18,19], assuming that their total energies  $E$  are far higher than the rest energy  $mc^2$ ,

$$E \gg mc^2, \quad (1)$$

and we discuss the mutual relations between our formulation and the Molière-Bethe formulation.

Let  $f(\theta, t)2\pi\theta d\theta$  be the azimuthally symmetric angular distribution of charged particles [26] with spatial deflection angle  $\theta$  after penetrating through uniform materials of thickness  $t$  measured in radiation length [3], and  $\tilde{f}(\zeta, t)$  be its double Fourier transform, or its Hankel transform under the azimuthally symmetric condition [18,19]

$$\tilde{f}(\zeta, t) = \frac{1}{2\pi} \iint e^{i\vec{\zeta} \cdot \vec{\theta}} \tilde{f}(\vec{\theta}, t) d\vec{\theta} = \int_0^\infty J_0(\zeta\theta) f(\theta, t) \theta d\theta, \quad (2)$$

$$f(\theta, t) = \frac{1}{2\pi} \iint e^{-i\vec{\theta} \cdot \vec{\zeta}} \tilde{f}(\vec{\zeta}, t) d\vec{\zeta} = \int_0^\infty J_0(\theta\zeta) \tilde{f}(\zeta, t) \zeta d\zeta. \quad (3)$$

According to our differential formulation, the diffusion equation for the Hankel transform  $\tilde{f}(\zeta, t)$  is expressed by a simple ordinary differential equation [27] under the small angle approximation

$$\frac{d\tilde{f}}{dt} = -\frac{K^2\zeta^2}{4E^2} \tilde{f} \left\{ 1 - \frac{1}{\Omega} \ln \frac{K^2\zeta^2}{4E^2} \right\}, \quad (4)$$

where  $\Omega$  and  $K$ , indicated in Tables III and IV later, denote the scattering constants showing the characteristics of material [18,19] discussed in Sec. IV B.

For normally incident charged particles under the fixed-energy condition (4) with the initial condition  $\tilde{f}=1/(2\pi)$  at  $t=0$  can be easily integrated as

$$\tilde{f} = \frac{1}{2\pi} \exp \left\{ -\frac{\theta_G^2\zeta^2}{4} \left( 1 - \frac{1}{\Omega} \ln \frac{\theta_G^2\zeta^2}{4t} \right) \right\}, \quad (5)$$

where

$$\theta_G^2 = K^2 t / E^2 \quad (6)$$

denotes the well-known Gaussian mean-square spatial angle for relativistic charged particles indicated in Eq. (1.55a) of Rossi and Greisen [3], only with  $E_s$  replaced by  $K$ . We can obtain the Molière angular distribution from Eq. (5) in double power series with  $\Omega^{-1}$  and  $\ln t$  as indicated in Appendix A. However, for derivation of the angular distribution, the more plain Molière's expression in simple power series with  $B^{-1}$  can be obtained from our solution [28]. According to the transport formula described in Appendix B, the solution (5) is changed to

$$\tilde{f} = \frac{1}{2\pi} \exp \left\{ -\frac{\theta_M^2\zeta^2}{4} \left( 1 - \frac{1}{B} \ln \frac{\theta_M^2\zeta^2}{4} \right) \right\}, \quad (7)$$

where the expansion parameter  $B$  and the scale angle  $\theta_M$  are derived from

$$B - \ln B = \Omega - \ln \Omega + \ln t, \quad (8)$$

$$\theta_M = \theta_G \sqrt{B/\Omega} \quad (9)$$

with  $\theta_G$  of Eq. (6), so that we have the Molière angular distributions  $f(\vartheta)2\pi\vartheta d\vartheta$  for spatial angle  $\theta$  and  $f_P(\varphi)d\varphi$  for projected angle  $\phi$ :

$$2\pi f(\vartheta) = f^{(0)}(\vartheta) + B^{-1}f^{(1)}(\vartheta) + B^{-2}f^{(2)}(\vartheta) + \cdots, \quad (10)$$

$$f_P(\varphi) = f_P^{(0)}(\varphi) + B^{-1}f_P^{(1)}(\varphi) + B^{-2}f_P^{(2)}(\varphi) + \cdots, \quad (11)$$

with the Molière series functions  $f^{(n)}(\vartheta)$  and  $f_P^{(n)}(\varphi)$  [12,13] and the scale variables

$$\vartheta = \theta/\theta_M \quad \text{and} \quad \varphi = \phi/\theta_M. \quad (12)$$

In actual cases, the energies of charged particles dissipate when the particles penetrate through the materials. If we assume continuous energy loss by ionization with a constant

TABLE I. The equation and the characteristic parameters of Molière angular distribution with ionization and their approximations.  $\alpha = zZ/(137\beta)$  denotes the Born parameter. Our results for charged particles of moderate energies give the traditional Molière results at the limit of  $\varepsilon \rightarrow 0$ , where an approximation of  $\beta'$  by  $\beta$  gives almost no differences in the resultant  $B$  and  $\theta_M$  for typical materials used in experiments. Our approximate results neglect the expansion terms of the order  $(mc^2/E)^4$  and higher. Moreover, our relativistic results neglect the terms of order  $(mc^2/E)^2$ .

Results for charged particles of moderate energies with ionization	
Equation	$\frac{d\tilde{f}}{z^2 dt} = -\frac{\xi^2}{w^2} \tilde{f} \left\{ 1 - \frac{1}{\Omega} \ln \frac{\beta'^2 \xi^2}{w^2} \right\}$
$\theta_G^2$	$\frac{K^2 z^2}{2\varepsilon mc^2} \left\{ \frac{mc^2}{pv} - \frac{mc^2}{p_0 v_0} + \frac{1}{2} \ln \frac{(E_0 - mc^2)(E - mc^2)}{(E_0 + mc^2)(E + mc^2)} \right\}$
$\ln \nu$	$\ln \frac{\beta'^2 \theta_G^2}{4z^2 t} - \frac{4z^2}{\theta_G^2} \int_0^t \frac{1}{w^2} \ln \frac{\beta'^2}{w^2} dt$
$B - \ln B$	$\Omega - \ln \Omega + \ln(\nu z^2 t / \beta^2)$
$\theta_M$	$\theta_G \sqrt{B/\Omega}$
Approximate results of $mc^2/E \ll 1$ and $\alpha^2 \ll 1$	
Equation	$\frac{d\tilde{f}}{z^2 dt} = -\frac{\xi^2}{w^2} \tilde{f} \left\{ 1 - \frac{1}{\Omega} \ln \frac{\beta^2 \xi^2}{w^2} \right\}$
$\theta_G^2$	$\frac{K^2 z^2 t}{E_0 E} \left\{ 1 + \frac{2m^2 c^4}{3E^2} \left( 1 + \frac{E}{E_0} + \frac{E^2}{E_0^2} \right) \right\}$
$\ln \nu$	$2 + \frac{E_0 + E}{E_0 - E} \ln \frac{E}{E_0} - \frac{m^2 c^4}{9E^2} \left( 14 + 5 \frac{E}{E_0} + 5 \frac{E^2}{E_0^2} + 12 \frac{E}{E_0} \frac{E_0 + E}{E_0 - E} \ln \frac{E}{E_0} \right)$
$B - \ln B$	$\Omega - \ln \Omega + \ln(\nu z^2 t / \beta^2)$
$\theta_M$	$\theta_G \sqrt{B/\Omega}$
Relativistic results of $mc^2/E \ll 1$ with $z=1$	
Equation	$\frac{d\tilde{f}}{dt} = -\frac{K^2 \xi^2}{4E^2} \tilde{f} \left\{ 1 - \frac{1}{\Omega} \ln \frac{K^2 \xi^2}{4E^2} \right\}$
$\theta_G^2$	$K^2 t / E_0 E$
$\ln \nu$	$2 + \frac{E_0 + E}{E_0 - E} \ln \frac{E}{E_0}$
$B - \ln B$	$\Omega - \ln \Omega + \ln(\nu t)$
$\theta_M$	$\theta_G \sqrt{B/\Omega}$

rate, the critical energy  $\varepsilon$  in unit radiation length [3,29], the incident particles of energy  $E_0$  lose their energies as

$$E = E_0 - \varepsilon t. \quad (13)$$

Then Eq. (4) becomes

$$\varepsilon \frac{d\tilde{f}}{dE} = \frac{K^2 \xi^2}{4E^2} \tilde{f} \left\{ 1 - \frac{1}{\Omega} \ln \frac{K^2 \xi^2}{4E^2} \right\}. \quad (14)$$

The solution satisfying the initial condition of  $\tilde{f}=1/(2\pi)$  at  $E=E_0$  is expressed by

$$\begin{aligned} \tilde{f} &= \frac{1}{2\pi} \exp \left\{ -\frac{K^2 \xi^2 t}{4E_0 E} \left[ 1 + \frac{1}{\Omega} \left( 2 + \frac{E_0 + E}{E_0 - E} \ln \frac{E}{E_0} \right) - \frac{1}{\Omega} \ln \frac{K^2 \xi^2}{4E_0 E} \right] \right\} \\ &= \frac{1}{2\pi} \exp \left\{ -\frac{\theta_G^2 \xi^2}{4} \left( 1 - \frac{1}{\Omega} \ln \frac{\theta_G^2 \xi^2}{4\nu t} \right) \right\}, \end{aligned} \quad (15)$$

where

$$\theta_G^2 = K^2 t / (E_0 E) \quad (16)$$

denotes the Gaussian mean-square spatial angle under the ionization process presented by Eyges [6], and

$$\nu = e^2 (E/E_0)^{(E_0+E)/(E_0-E)} \quad (17)$$

denotes a newly introduced factor under the ionization process, agreeing with Molière's evaluation [30].  $\nu$  is a function of the fractional energy  $E/E_0$  or the fractional dissipation  $(E_0 - E)/E_0$ , decreasing from 1 to 0 as the fraction of dissipated energy increases from 0 to 1, as indicated by the solid curve in Fig. 2 in the next section.

According to our transport formula introduced in Appendix B, solution (15) can be expressed as Eq. (7). Thus we get the Molière angular distribution with ionization in the simple series of Eq. (10), where the expansion parameter  $B$  is determined from

$$B - \ln B = \Omega - \ln \Omega + \ln(\nu t) \quad (18)$$

and the scale angle  $\theta_M$  from Eq. (9) with (16), as listed in Table I. Variations in the expected angular distribution with energy dissipation for relativistic muons are compared with those under the fixed-energy condition in Fig. 1.

Eyges found that the angular distribution under the Gaussian approximation with ionization loss of a constant rate is easily obtained from the distribution without ionization simply by replacing the energy  $E$  with the geometrical mean between the incident and the destination  $\sqrt{E_0 E}$  [6]. However, we find that the Molière angular distribution with ionization for relativistic particles is instead obtained from traditional results without ionization by replacing both the thickness  $t$  and the energy  $E$  with the effective variables  $\nu t$  and  $\sqrt{\nu E_0 E}$  as the characteristic parameters  $B$  and  $\theta_M$  obey this rule as confirmed in Eqs. (9), (16), and (18). The thickness is reduced to the effective value of  $\nu t$  under the ionization process, so we can call  $\nu$  the contraction factor. The expansion parameter  $B$  increases more slowly compared with  $B$  under the fixed-energy process due to the slower increase of  $\nu t$ , and moreover  $B$  begins to decrease at the last stage of traverse along with the decrease of the value  $\nu t$  in Eq. (18).

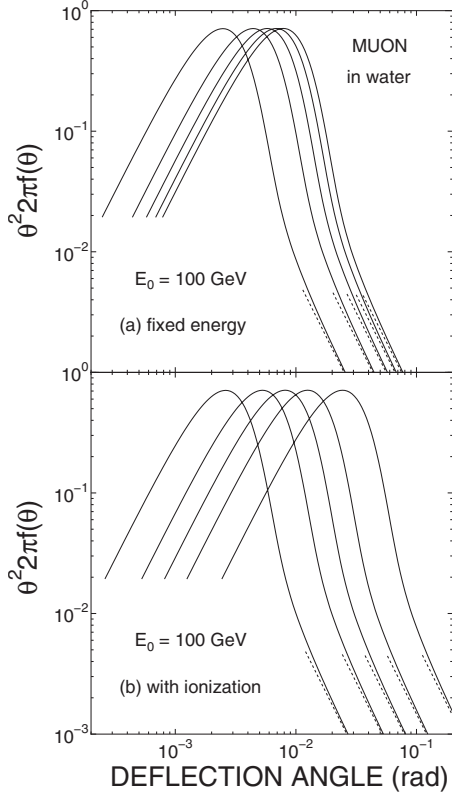


FIG. 1. Comparison of expected angular distributions multiplied by  $\theta^2$  for muons with and without ionization loss, assuming that rest energy is negligible. Solid curves in (b) show the distributions after 39.3, 118, 197, 275, and 354 m traverses in water with ionization, from left to right, where the incident muons dissipate 10, 30, 50, 70, and 90 % of their initial energies. The curves in (a) show the distributions after the same traverses without ionization. Dotted curves indicate accumulations of the single-scattering distribution integrated over the traversed thickness as evaluated in Eq. (106).

### III. MOLIÈRE DISTRIBUTIONS WITH IONIZATION FOR LINEAR COMBINATION BETWEEN THE DEFLECTION ANGLE AND THE LATERAL DISPLACEMENT

Molière obtained the generalized distribution for linear combination between the deflection angle  $\vec{\theta}$  and the lateral displacement  $\vec{r}$  under the fixed-energy condition [16]. We improve on his result to take account of ionization loss in Eq. (13), for relativistic charged particles.

Let the simultaneous distribution between  $\vec{\theta}$  and  $\vec{r}$  be  $f(\vec{\theta}, \vec{r}, t) d\vec{\theta} d\vec{r}$  and its Fourier transform be  $\tilde{f}(\vec{\zeta}, \vec{\eta}, t)$ :

$$f(\vec{\theta}, \vec{r}, t) = \frac{1}{4\pi^2} \int \int \int e^{-i\vec{\theta}\cdot\vec{\zeta} - i\vec{r}\cdot\vec{\eta}} \tilde{f}(\vec{\zeta}, \vec{\eta}, t) d\vec{\zeta} d\vec{\eta}, \quad (19)$$

where  $\vec{\zeta}$  and  $\vec{\eta}$  denote the Fourier variables corresponding to  $\vec{\theta}$  and  $\vec{r}$ , respectively. The diffusion equation for Fourier transform of the simultaneous distribution is described as

$$\frac{\partial \tilde{f}}{\partial t'} = \vec{\eta} \frac{\partial \tilde{f}}{\partial \vec{\zeta}'} - \frac{K^2 \zeta'^2}{4E'^2} \tilde{f} \left\{ 1 - \frac{1}{\Omega} \ln \frac{K^2 \zeta'^2}{4E'^2} \right\}, \quad (20)$$

where the variables  $\vec{\zeta}'$  and  $E'$  change together with the differential variable  $t'$ . The first term of the right-hand side vanishes when we replace the variable  $\vec{\zeta}'$  as

$$\vec{\zeta}' = \vec{\zeta} + (t - t') \vec{\eta}, \quad (21)$$

where  $t$  and  $\vec{\zeta}$  denote the destination thickness and Fourier variable. Then Eq. (20) can be integrated as

$$\begin{aligned} \ln 4\pi^2 \tilde{f} &= - \int_0^t \frac{K^2 \zeta'^2}{4E'^2} \left\{ 1 - \frac{1}{\Omega} \ln \frac{K^2 \zeta'^2}{4E'^2} \right\} dt' \\ &= \int_0^1 \frac{K^2 t (\vec{\zeta} + \vec{\eta} t u)^2}{4\Omega (E + \varepsilon t u)^2} \ln \frac{K^2 (\vec{\zeta} + \vec{\eta} t u)^2}{4e^\Omega (E + \varepsilon t u)^2} du, \end{aligned} \quad (22)$$

where  $E$  denotes the destination energy.

Let  $\vec{\rho}$  be the linear combination between the deflection angle  $\vec{\theta}$  and the lateral displacement  $\vec{r}$ , or the chord angle  $\vec{r}/t$  [2,16], with respective weights of  $a$  and  $b$ ,

$$\vec{\rho} = a\vec{\theta} + b\vec{r}/t, \quad (23)$$

and  $g(\vec{\rho}, t)$  be its probability density [31]. For  $b=0$ , the problem is reduced to the angular distribution described in the previous section. For  $b \neq 0$ , we have

$$g(\vec{\rho}, t) d\vec{\rho} = \frac{t d\vec{\rho}}{b} \iint f\left(\vec{\theta}, \frac{t}{b}(\vec{\rho} - a\vec{\theta}), t\right) d\vec{\theta}, \quad (24)$$

so that the Fourier transform  $\tilde{g}(\vec{\xi}, t)$  of  $g(\vec{\rho}, t)$ ,

$$\tilde{g}(\vec{\xi}) = \frac{1}{2\pi} \iint e^{-i\vec{\xi}\cdot\vec{\rho}} g(\vec{\rho}, t) d\vec{\rho} = 2\pi \tilde{f}(a\vec{\xi}, b\vec{\xi}/t, t), \quad (25)$$

is derived as

$$\begin{aligned} \ln 2\pi \tilde{g} &= \int_0^1 \frac{K^2 t \xi^2 (a + bu)^2}{4\Omega (E + \varepsilon t u)^2} \ln \frac{K^2 \xi^2 (a + bu)^2}{4e^\Omega (E + \varepsilon t u)^2} du \\ &= \int_E^{E_0} \frac{b^2 K^2 t \xi^2}{4\Omega \varepsilon^3 t^3} \left(1 - \frac{Q}{E'}\right)^2 \ln \left[ \frac{b^2 K^2 \xi^2}{4e^\Omega \varepsilon^2 t^2} \left(1 - \frac{Q}{E'}\right)^2 \right] dE' \\ &= \int_{Q/E_0}^{Q/E} \frac{b^2 Q K^2 t \xi^2}{4\Omega \varepsilon^3 t^3} \left(1 - \frac{1}{s}\right)^2 \ln \frac{b^2 K^2 \xi^2 (1-s)^2}{4e^\Omega \varepsilon^2 t^2} ds \\ &= - \frac{b^2 Q K^2 t \xi^2}{4\Omega (E_0 - E)^3} \left\{ 2 \left[ s + \ln|s| - \left(s - \frac{1}{s}\right) \ln|1-s| \right. \right. \\ &\quad \left. \left. - 2\mathcal{L}_2(s) \right]_{Q/E_0}^{Q/E} - \left[ s - \frac{1}{s} - 2 \ln|s| \right]_{Q/E}^{Q/E} \right. \\ &\quad \left. \times \ln \frac{b^2 K^2 \xi^2}{4e^\Omega (E_0 - E)^2} \right\}, \end{aligned} \quad (26)$$

where we define

$$Q \equiv E - (a/b)\varepsilon t, \quad (27)$$

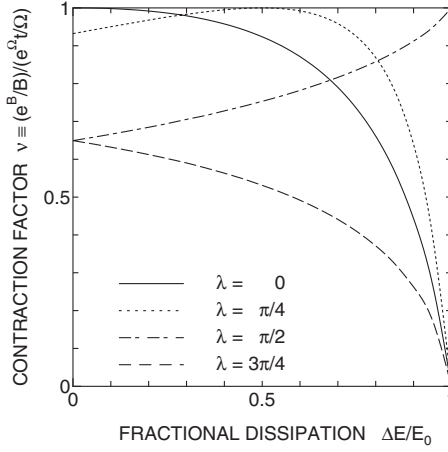


FIG. 2. The contraction factors  $\nu$ , or the ratios of  $e^B/B$  to  $e^{\Omega t}/\Omega$ , for the combination angle  $\vec{\rho} \equiv \vec{\theta} \cos \lambda + (\vec{r}/t) \sin \lambda$  under the ionization process defined for relativistic charged particles. Abscissa denotes the fraction of dissipated energy  $(E_0 - E)/E_0$ .

$$[h(s)]_x^y \equiv h(y) - h(x), \quad (28)$$

and  $\mathcal{L}_2(z)$  denotes the dilogarithm function [32,33]

$$\mathcal{L}_2(z) = \int_z^0 \frac{\ln|1-t|}{t} dt. \quad (29)$$

According to our transport formula introduced in Appendix B, solution (26) can be expressed as Eq. (7), so that we can describe both the spatial and the projected distributions for  $\vec{\rho}$  in Molière series of Eqs. (10) and (11) with the expansion parameter  $B$  expressed by Eq. (18) and the scale angle  $\theta_M$  expressed by Eq. (9), where the contraction factor  $\nu$  in this case is determined as

$$\ln \nu = \frac{2[s + \ln|s| - (s - s^{-1})\ln|1-s| - 2\mathcal{L}_2(s)]_{Q/E_0}^{Q/E}}{[s - s^{-1} - 2\ln|s|]_{Q/E_0}^{Q/E}} + \ln \frac{Q[s - s^{-1} - 2\ln|s|]_{Q/E_0}^{Q/E}}{E_0 - E} \quad (30)$$

and the mean-square Gaussian angle  $\theta_G^2$  are determined as

$$\theta_G^2 = \frac{b^2 Q K^2 t}{(E_0 - E)^3} \left[ s - \frac{1}{s} - 2\ln|s| \right]_{Q/E_0}^{Q/E} \equiv \mu^2 \frac{K^2 t}{E_0^2}. \quad (31)$$

We have introduced square of the broadening factor  $\mu^2$  to give the ratio of the Gaussian mean-square angle  $\theta_G^2$  for the combination angle  $\vec{\rho}$  under the ionization process (31) to  $\theta_G^2$  for the deflection angle  $\vec{\theta}$  under the fixed-energy process (6), for the sake of geometrical understanding. We indicate the values of  $\nu$  in Fig. 2 and Table II as well as the values of  $\mu^2$  in Fig. 3, taking  $a = \cos \lambda$  and  $b = \sin \lambda$  as Molière did [16]. Both factors  $\nu$  and  $\mu$  are functions of the fraction of residual energy  $E/E_0$  or functions of the fraction of dissipated energy  $\Delta E/E_0$ . In  $\nu$  from Fig. 2 at  $\Delta E/E_0 = 0$  and  $\mu^2$  of Fig. 3 at  $E/E_0 = 1$  agree with Molière's results without ionization [16] in the fourth and the third rows of his Table 1, respectively [34]. Our factors at the limit of  $E \rightarrow 0$  have nonzero finite

TABLE II. The contraction factor  $\nu$  for the linear combination  $\vec{\rho} = \vec{\theta} \cos \lambda + (\vec{r}/t) \sin \lambda$ .  $\Delta E/E_0 = (E_0 - E)/E_0$  denotes the fraction of the dissipated energy.

$\Delta E/E_0$	$\lambda = 0$	$\lambda = \pi/4$	$\lambda = \pi/2$	$\lambda = 3\pi/4$
0.00	1.0000	0.9320	0.6492	0.6492
0.05	0.9996	0.9412	0.6575	0.6409
0.10	0.9982	0.9502	0.6662	0.6320
0.15	0.9956	0.9590	0.6752	0.6225
0.20	0.9917	0.9677	0.6846	0.6124
0.25	0.9863	0.9760	0.6945	0.6016
0.30	0.9791	0.9829	0.7054	0.5902
0.35	0.9696	0.9895	0.7157	0.5772
0.40	0.9576	0.9949	0.7278	0.5632
0.45	0.9425	0.9986	0.7400	0.5481
0.50	0.9236	1.0000	0.7531	0.5310
0.55	0.9002	0.9982	0.7670	0.5126
0.60	0.8711	0.9921	0.7821	0.4917
0.65	0.8349	0.9797	0.7986	0.4680
0.70	0.7898	0.9583	0.8164	0.4409
0.75	0.7331	0.9236	0.8360	0.4091
0.80	0.6609	0.8686	0.8580	0.3711
0.85	0.5674	0.7811	0.8829	0.3240
0.90	0.4430	0.6390	0.9122	0.2625
0.95	0.2695	0.3986	0.9482	0.1740
1.00	0.0000	0.0000	1.0000	0.0000

values only for the chord-angle distribution or the lateral distribution ( $\lambda = \pi/2$ ), and thus practically provide the probability density.

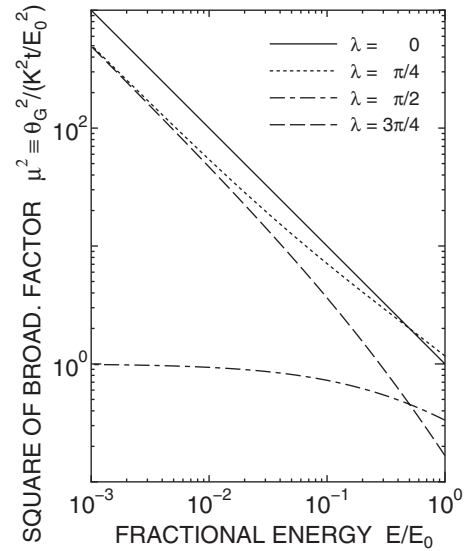


FIG. 3. Square of the broadening factor  $\mu^2$  or the ratios of the Gaussian mean square angle  $\theta_G^2$  for the combination angle  $\vec{\rho} \equiv \vec{\theta} \cos \lambda + (\vec{r}/t) \sin \lambda$  to  $K^2 t/E_0^2$ , under the ionization process defined for relativistic charged particles. Abscissa denotes the fraction of residual energy  $E/E_0$ .

At the limit of  $\varepsilon \rightarrow 0$ , Eq. (18) with Eqs. (30) and (31) gives the characteristic parameters  $B$  and  $\theta_M$  for the combination-angle distribution under the fixed-energy condition

$$B - \ln B = \Omega - \ln \Omega + \ln t + \frac{2}{3} + \frac{a^3/b}{3a^2 + 3ab + b^2} \ln \frac{a^2}{(a+b)^2} + \ln \frac{3a^2 + 3ab + b^2}{3(a+b)^2}, \quad (32)$$

$$\frac{\theta_M^2}{B} = \frac{3a^2 + 3ab + b^2}{3} \frac{K^2 t}{\Omega E^2}, \quad (33)$$

which agree with Molière's results (3.11b) and (3.15) [16]. Meanwhile under the special case of  $a/b = E/(\varepsilon t)$ , including the case of  $\vec{\rho} \rightarrow \vec{r}/t$  with  $E \rightarrow 0$ , Eq. (26) can be easily integrated within an elementary function as

$$\ln 2\pi\tilde{g} = \frac{(a+b)^2 K^2 t \xi^2}{4\Omega E_0^2} \ln \frac{(a+b)^2 K^2 t \xi^2}{4e^{\Omega} E_0^2}, \quad (34)$$

so we find from Eqs. (B2) and (B5) that the distribution for linear combination  $\vec{\rho}$  under this condition has the same Molière distribution as the angular distribution without ionization loss, except with the scale angle  $\theta_M$  of  $(a+b)$  times large or small value.

#### IV. MOLIÈRE ANGULAR DISTRIBUTION WITH IONIZATION FOR CHARGED PARTICLES OF MODERATE ENERGIES

We construct in this section the differential formulation of the Molière theory applicable to charged particles of moderate energies, taking account of the rest energy of penetrating particles, and apply our formulation to Goudsmit-Saunderson angular distribution with ionization. We also define the scattering constants that are applicable even to these particles and evaluate them so that they are consistent with the Table of Atomic and Nuclear Properties of Materials in *The Review of Particle Physics* [24].

##### A. The diffusion equation for charged particles of moderate energies

Let  $f(\vec{\theta}, x) d\vec{\theta}$  be the angular distribution of charged particles having traversed through uniform materials of thickness  $x$  measured in g/cm<sup>2</sup>. Under the condition of continuous energy loss without fluctuation, the diffusion equation for the angular distribution is described as [13,18,19]

$$\frac{d}{dx} f(\vec{\theta}, x) = \frac{N}{A} \int \int \{f(\vec{\theta} - \vec{\theta}', x) - f(\vec{\theta}, x)\} \sigma(\vec{\theta}') d\vec{\theta}', \quad (35)$$

where  $A$  denotes the atomic weight,  $N$  the Avogadro constant, and  $\sigma(\theta)$  the screened single-scattering formula under the small angle approximation [2]

$$\sigma(\theta) 2\pi\theta d\theta = \frac{4z^2 Z(Z+1)e^4}{p^2 v^2} \theta^{-4} 2\pi\theta d\theta, \quad \theta > \sqrt{e}\chi_a, \quad (36)$$

where  $p$  denotes the momentum and  $v$  the velocity of particles with charge  $z$  penetrating through material of atomic number  $Z$ , and  $\chi_a$  the characteristic screening angle [11,13]. Applying Hankel transform of Eq. (2), we have the equation under the azimuthally symmetric condition

$$\begin{aligned} d\tilde{f} &= -2\pi \frac{N}{A} \tilde{f} dx \int_0^\infty [1 - J_0(\zeta\theta)] \sigma(\theta) \theta d\theta \\ &= -\frac{K^2 2z^2 dt}{\Omega p^2 v^2 \tilde{f}} \int_{\sqrt{e}\chi_a}^\infty [1 - J_0(\zeta\theta)] \theta^{-3} d\theta, \end{aligned} \quad (37)$$

where  $t$  denotes the traversed thickness measured in units of radiation length  $X_0$  [3,29,35,36],

$$t \equiv x/X_0, \quad (38)$$

and we introduced the scattering constants  $\Omega$  and  $K$  satisfying

$$\frac{K^2}{\Omega} \equiv \frac{N}{137A} E_s^2 r_e^2 Z(Z+1) X_0, \quad (39)$$

where  $r_e$  denotes the classical electron radius and  $E_s = \sqrt{4\pi \times 137 m_e c^2} \approx 21.2$  MeV denotes the scale energy [3,24].

The integration on the right-hand side of Eq. (37) can be evaluated by using the formula [2,13]

$$I_1(x) \equiv 4 \int_x^\infty t^{-3} [1 - J_0(t)] dt = 1 + \ln 2 - C - \ln x + O(x^2), \quad (40)$$

where  $C=0.57721\cdots$  is Euler's constant. So we can describe the equation as

$$\begin{aligned} \frac{d\tilde{f}}{z^2 dt} &= -\frac{K^2}{2\Omega} \frac{\xi^2}{p^2 v^2} \tilde{f} \{1 + \ln 2 - C - \ln(\sqrt{e}\chi_a \xi)\} \\ &= -\frac{1}{\Omega} \frac{K^2 \xi^2}{4p^2 v^2} \tilde{f} \left\{ \ln \frac{\beta^2 K^2 / (p^2 v^2 \chi_0^2)}{e^{2C-1} [\chi_a^2 / \chi_0^2]_{\text{rel}}} \right. \\ &\quad \left. - \ln \frac{\beta^2 \chi_a^2 / \chi_0^2}{[\chi_a^2 / \chi_0^2]_{\text{rel}}} - \ln \left( \frac{K^2 \xi^2}{4p^2 v^2} \right) \right\}, \end{aligned} \quad (41)$$

where  $\chi_0$  denotes the angular constant [11,13]

$$\chi_0 = \hbar/(ap), \quad (42)$$

with  $a$  as the Thomas-Fermi radius of the atom [11] and  $[\chi_a^2 / \chi_0^2]_{\text{rel}}$  is defined as the value of  $\chi_a^2 / \chi_0^2$  for singly charged particles with relativistic energies of Eq. (1). Now we can take  $\Omega$  as the first term in the bracket of the right-hand side of Eq. (41),

$$\Omega \equiv \ln \frac{K^2/(p^2 c^2 \chi_0^2)}{e^{2C-1}[\chi_a^2/\chi_0^2]_{\text{rel}}}, \quad (43)$$

then our scattering constants  $\Omega$  and  $K$ , defined by Eqs. (39) and (43), become specific to material, and the diffusion equation (41) to give the Hankel transform of the Molière angular distribution for charged particles of moderate energies becomes simple:

$$\frac{d\tilde{f}}{z^2 dt} = -\frac{\xi^2}{w^2} \tilde{f} \left\{ 1 - \frac{1}{\Omega} \ln \frac{\beta'^2 \xi^2}{w^2} \right\}, \quad (44)$$

where

$$w \equiv 2pv/K \quad (45)$$

is the parameter defined in Rossi and Greisen [3], except that the scale energy  $E_s$  is replaced by our  $K$  and

$$\beta'^2 = \frac{\chi_a^2/\chi_0^2}{[\chi_a^2/\chi_0^2]_{\text{rel}}} \beta^2 \quad (46)$$

is a factor to act for multiply charged ( $z > 1$ ) and/or nonrelativistic particles and to take 1 for singly charged relativistic particles. It will be helpful in later analyses to express the single-scattering formula and the characteristic screening angle of Eqs. (36) and (46) by our scattering constants  $\Omega$  and  $K$  determined from Eqs. (39) and (43):

$$\frac{N}{A} \sigma(\theta) 2\pi \theta d\theta dx = \frac{1}{\pi \Omega} \frac{K^2 z^2}{p^2 v^2} \theta^{-4} 2\pi \theta d\theta dt, \quad (47)$$

$$\chi_a^2 = \frac{\beta'^2 K^2}{p^2 v^2} e^{-\Omega+1-2C}. \quad (48)$$

### B. The scattering constants for pure material under the Molière screening model

Molière evaluated the screening angle [11,13] as

$$\chi_a^2 = (1.13 + 3.76\alpha^2)\chi_0^2, \quad (49)$$

where

$$\alpha \equiv zZ/(137\beta) \quad (50)$$

denotes the so-called Born parameter [2] for charged particles. Then we can determine the values of  $\Omega$  and  $K$  specific to materials from Eqs. (39) and (43), to be consistent with the Table of Atomic and Nuclear Properties of Materials in *The Review of Particle Physics* [24]:

$$\begin{aligned} \Omega - \ln \Omega &= \ln \frac{4\pi N r_e^2 Z(Z+1)(0.885Z^{-1/3})^2 X_0}{e^{2C-1}(1.13 + 3.76Z^2/137^2)A/137^2} \\ &= \ln \frac{6700(Z+1)Z^{1/3}X_0}{(1 + 3.34Z^2/137^2)A}, \end{aligned} \quad (51)$$

$$K^2 = 3.49 \times 10^{-4} Z(Z+1)X_0 \Omega E_s^2/A, \quad (52)$$

as listed in Table III. Note that the right-hand side of our Eq. (51) shows the logarithm of Bethe's equation (22) [13] with

TABLE III. The scattering constants  $\Omega$  and  $K$  defined in Sec. IV B under the Molière screening model for pure materials revised to be consistent with the Table of Atomic and Nuclear Properties of Materials in *The Review of Particle Physics* [24]. Radiation lengths  $X_0$  are taken from Tsai [36]. Critical energies  $\varepsilon$  are taken from smoothed formulas, 710 MeV/( $Z+0.92$ ) for gases and 610 MeV/( $Z+1.24$ ) for solids and liquids [24].

Material	Z	A	$X_0$ (g/cm <sup>2</sup> )	$\varepsilon$ (MeV)	$\Omega$	K (MeV)
H	1	1.008	63.05	369.8	16.44	17.96
He	2	4.003	94.32	243.2	16.07	18.88
Li	3	6.941	82.76	143.9	15.80	18.83
C	6	12.011	42.70	84.3	15.34	18.96
N	7	14.007	37.99	89.7	15.25	19.06
O	8	15.999	34.24	79.6	15.17	19.15
Na	11	22.990	25.74	49.8	14.89	18.58
Al	13	26.982	24.01	42.8	14.85	19.43
Si	14	28.086	21.82	40.0	14.80	19.47
S	16	32.066	19.50	35.4	14.71	19.54
Ar	18	39.948	19.55	37.5	14.63	19.60
Fe	26	55.845	13.84	22.4	14.34	19.79
Cu	29	63.546	12.86	20.2	14.25	19.84
Ge	32	72.610	12.25	18.4	14.17	19.90
Br	35	79.904	11.42	16.8	14.08	19.94
Ag	47	107.87	8.970	12.7	13.77	20.13
I	53	126.90	8.480	11.3	13.62	20.22
Cs	55	132.91	8.305	10.9	13.58	20.25
W	74	183.84	6.763	8.11	13.15	20.52
Pb	82	207.20	6.369	7.72	12.99	20.65
Bi	83	208.98	6.290	7.24	12.97	20.67

$z=1$ ,  $\beta=1$ , and his  $t$  of  $X_0$ , giving  $e^{2-2C}$  times the number of collisions in the unit radiation length. Then  $\theta_M$  of our Eq. (9) becomes  $\theta_G$  of  $K/E$ , and we find our scattering constants  $\Omega$  and  $K$  denote  $B$  and  $E\theta_M$  for singly charged relativistic particles after penetrating the unit radiation length.

### C. The angular distribution for charged particles of moderate energies with ionization

We derive the Molière angular distribution for charged particles of moderate energies with ionization. The diffusion equation (44) can be solved as

$$\tilde{f} = \frac{1}{2\pi} \exp \left\{ -\frac{\theta_G^2 z^2}{4} \left( 1 - \frac{1}{\Omega} \ln \frac{\beta'^2 \theta_G^2 z^2}{4\nu z^2 t} \right) \right\}, \quad (53)$$

where

$$\theta_G^2 = \int_0^t \frac{4z^2}{w^2} dt \quad (54)$$

denotes the Gaussian mean-square angle with  $E_s$  replaced by  $K$ , and  $\nu$  derived by

$$\ln \frac{\nu}{\beta'^2} = \ln \frac{\theta_G^2}{4z^2 t} - \frac{4z^2}{\theta_G^2} \int_0^t \frac{1}{w^2} \ln \frac{\beta'^2}{w^2} dt \quad (55)$$

denotes the contraction factor for charged particles of moderate energies. Especially under the ionization process with a constant dissipation rate of  $\varepsilon z^2$  in each radiation length

$$E = E_0 - \varepsilon z^2 t, \quad (56)$$

Eq. (54) becomes

$$\theta_G^2 = \frac{K^2}{2\varepsilon mc^2} \left\{ \frac{mc^2}{pv} - \frac{mc^2}{p_0 v_0} + \frac{1}{2} \ln \frac{(E_0 - mc^2)/(E - mc^2)}{(E_0 + mc^2)/(E + mc^2)} \right\}. \quad (57)$$

Thus the spatial and projected angular distributions are determined by the Molière series (10) and (11) with the expansion parameter  $B$  derived from

$$B - \ln B = \Omega - \ln \Omega + \ln(\nu z^2 t / \beta'^2) \quad (58)$$

and the scale angle  $\theta_M$  derived from Eq. (9) with (54), as listed in Table I.

Under the relativistic condition of Eq. (1), we have

$$\beta'^2 \simeq \frac{1 + 3.34z^2 Z^2 / 137^2}{1 + 3.34Z^2 / 137^2}. \quad (59)$$

So we can obtain the Molière angular distribution from the expansion parameter  $B$  derived from

$$B - \ln B \simeq \Omega - \ln \Omega + \ln \left( \frac{1 + 3.34Z^2 / 137^2}{1 + 3.34z^2 Z^2 / 137^2} \nu z^2 t \right) \quad (60)$$

and the scale angle  $\theta_M$  derived from Eq. (9) with Eq. (16). Equation (60) for relativistic charged particles is reduced to Eq. (18) for singly charged particles.

Under the condition that the Born parameter is small enough as

$$\alpha \equiv zZ / (137\beta) \ll 1, \quad (61)$$

it satisfies

$$\beta' \simeq \beta. \quad (62)$$

Then with  $\beta'$  approximated by  $\beta$ ,  $B$  can be determined simply as

$$B - \ln B \simeq \Omega - \ln \Omega + \ln(\nu z^2 t / \beta^2) \quad (63)$$

instead of Eq. (58), and  $\nu$  is derived numerically, e.g., from the partial integration of Eq. (55):

$$\ln \nu = \ln \frac{\theta_G^2 p^2 v^2}{K^2 z^2 t} - \frac{2z^2 \varepsilon}{\theta_G^2} \int_0^t \frac{\theta_G^2}{pv} dt. \quad (64)$$

In Fig. 4 we compare the resultant characteristic parameters  $B$  and  $\theta_M$  of charged particles with various rest energies, approximating  $\beta'$  by  $\beta$  with Eqs. (63), (9), and (57). Values of the parameters  $B$  and  $\theta_M$  begin to deviate significantly from those derived under the fixed-energy condition (thin solid line), while their total energies dissipate until they approach the rest energies.

We also examine whether or not the condition  $\beta' \simeq \beta$  satisfies the typical materials used in experiments.  $B$  and  $\theta_M$ ,

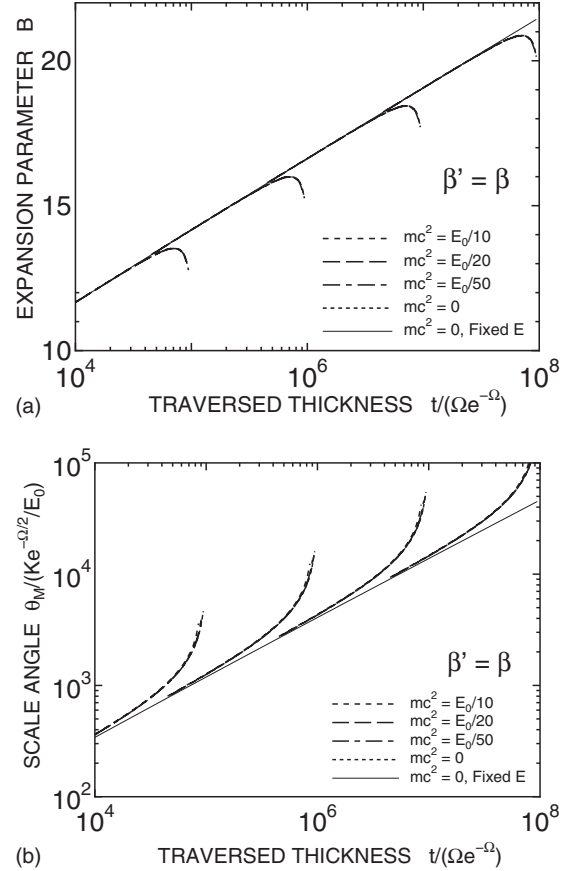


FIG. 4. The values of the expansion parameters  $B$  (a) and the scale angles  $\theta_M$  (b) begin to deviate significantly from those derived under the fixed-energy condition (thin solid lines), along with dissipating their energies and approaching to their rest energies. Differences due to the different rest energies are small (thick lines). The unit of abscissa,  $\Omega e^{-\Omega}$  of the order of  $10^{-6}$  radiation length, denotes  $e^{2C-2}$  times the mean-free path of Eq. (107) of the single scattering for relativistic charged particles, and the unit of  $\theta_M$  ordinate  $Ke^{-\Omega/2}/E_0$  denotes  $e^{C-1}$  times the screening angle  $\sqrt{e}\chi_a$  of the incident charged particle. The four branches of the curve correspond to the incident energies  $E_0$  of  $10^5$ ,  $10^6$ ,  $10^7$ , and  $10^8$  from left to right, in units of  $\Omega e^{-\Omega}\varepsilon$ .

exactly derived from  $\beta'$  of Eqs. (58) and (9) with Eq. (57), are compared with those conventionally derived approximating  $\beta'$  by  $\beta$ , on materials C, Fe, and Pb in Fig. 5. We confirm that there are almost no visible differences of more than 0.1 percent between the results from  $\beta'$  and  $\beta$  within the traversed thickness of an energy loss of less than 70%.

#### D. Applications of our differential formulation to Goudsmit-Saunderson angular distribution with ionization

The Goudsmit-Saunderson theory of multiple Coulomb scattering [9,10] accurately traces the deflection angle without using the small angle approximation [2]. We propose a convenient method to derive Goudsmit-Saunderson series terms by applying our Molière theory with ionization.

According to Lewis [15], the probability density of Goudsmit-Saunderson angular distribution  $f_{GS}(\theta, t)2\pi \sin \theta d\theta$  is expressed as

$$\begin{aligned}
 2\pi f_{\text{GS}}(\theta, t) &= \sum_{l=0}^{\infty} \left( l + \frac{1}{2} \right) P_l(\cos \theta) \exp \left\{ - \int_0^x dx \int_0^{\pi} 2\pi \frac{N}{A} \sigma(\theta) \right. \\
 &\quad \left. \times [1 - P_l(\cos \theta)] \sin \theta d\theta \right\}, \\
 &\equiv \sum_{l=0}^{\infty} \left( l + \frac{1}{2} \right) P_l(\cos \theta) \exp \left\{ - \int_0^x \kappa dx \right\}. \quad (65)
 \end{aligned}$$

Evaluating the exponent as Lewis did by substituting the single-scattering formula (47) and the screening angle (48), we have

$$\begin{aligned}
 - \int_0^x \kappa dx &= - \int_0^t \frac{2K^2 z^2 dt}{\Omega p^2 v^2} \int_{-1}^1 \frac{1 - P_l(\mu)}{4(1 - \mu + \chi_a^2/2)^2} d\mu \\
 &\approx - \int_0^t \frac{K^2 z^2 dt}{4\Omega p^2 v^2} l(l+1) \left( 1 - \ln \frac{\chi_a^2}{4} - 2 \sum_{m=1}^l m^{-1} \right) \\
 &= - \int_0^t \frac{K^2 z^2 dt}{4p^2 v^2} l(l+1) \left( 1 - \frac{1}{\Omega} \left[ \ln \frac{\beta'^2 K^2}{4p^2 v^2} - 2C \right. \right. \\
 &\quad \left. \left. + 2 \sum_{m=1}^l m^{-1} \right] \right) \\
 &= - \frac{\theta_G^2}{4} l(l+1) \left( 1 - \frac{1}{\Omega} \left[ \ln \frac{\beta'^2 \theta_G^2}{4\nu z^2 t} + 2\psi(l+1) \right] \right) \\
 &= - \frac{\theta_M^2}{4} l(l+1) \left( 1 - \frac{1}{B} \left[ \ln \frac{\theta_M^2}{4} + 2\psi(l+1) \right] \right), \quad (66)
 \end{aligned}$$

where  $\psi(z) = (d/dz) \ln \Gamma(z)$  denotes the psi function [32], the Gaussian mean-square angle  $\theta_G^2$  and the contraction factor  $\nu$  are derived as Eqs. (54) and (55), and the characteristic parameters  $B$  and  $\theta_M$  of Eqs. (58) and (9) are the same as those derived in the preceding subsection under the Molière theory. So we obtain the Goudsmit-Saunderson angular distribution with ionization

$$\begin{aligned}
 2\pi f_{\text{GS}}(\theta, t) &= \sum_{l=0}^{\infty} \left( l + \frac{1}{2} \right) P_l(\cos \theta) \exp \left\{ - \frac{\theta_M^2}{4} l(l+1) \right. \\
 &\quad \left. \times \left( 1 - \frac{1}{B} \left[ \ln \frac{\theta_M^2}{4} + 2\psi(l+1) \right] \right) \right\}, \quad (67)
 \end{aligned}$$

corresponding to the Molière angular distribution  $f_M(\theta, t) 2\pi \theta d\theta$  with ionization

$$2\pi f_M(\theta, t) = \int_0^{\infty} \zeta d\zeta J_0(\theta \zeta) \exp \left\{ - \frac{\theta_M^2 \zeta^2}{4} \left( 1 - \frac{1}{B} \ln \frac{\theta_M^2 \zeta^2}{4} \right) \right\}, \quad (68)$$

using the same characteristic parameters  $B$  and  $\theta_M$ .

Determined from  $B$  and  $\theta_M$ , the Goudsmit-Saunderson angular distribution for relativistic charged particles with a constant ionization loss rate is also derived from the results without ionization only by replacing the thickness  $t$  and the

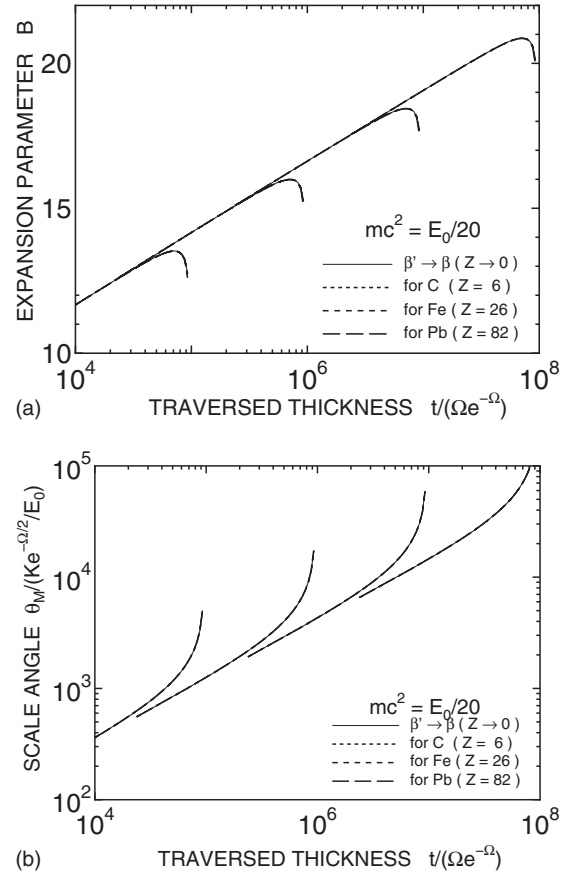


FIG. 5. Differences due to the different materials are small among the expansion parameters  $B$  (a) and the scale angles  $\theta_M$  (b) vs traversed thickness (thick lines). The four branches of the curve correspond to the incident energies  $E_0$  of  $10^5$ ,  $10^6$ ,  $10^7$ , and  $10^8$  from left to right, in units of  $\Omega e^{-\Omega} \epsilon$ , where the rest energies are all assumed to be  $E_0/20$ .

energy  $E$  with the effective thickness  $\nu t$  and energy  $\sqrt{\nu E_0 E}$ , as in the Molière angular distribution investigated in Sec. II. The Goudsmit-Saunderson angular distribution thus derived is compared with the Molière angular distribution in Fig. 6 under both the fixed-energy and ionization processes. We found almost no differences between them within angular ranges that satisfy the small-angle approximation.

#### E. An approximate method to express the contraction factor $\nu$ for charged particles of moderate energy

We derive an approximate expression of the contraction factor  $\nu$  from expansion of Eqs. (57) and (64) with  $mc^2/E$  up to the second order. As it holds that

$$\nu = E \left( 1 - \frac{m^2 c^4}{E^2} \right), \quad (69)$$

$$\theta_G^2 \approx \frac{K^2 z^2 t}{E_0 E} \left\{ 1 + \frac{2}{3} \frac{m^2 c^4}{E^2} \left( 1 + \frac{E}{E_0} + \frac{E^2}{E_0^2} \right) \right\}, \quad (70)$$

we have

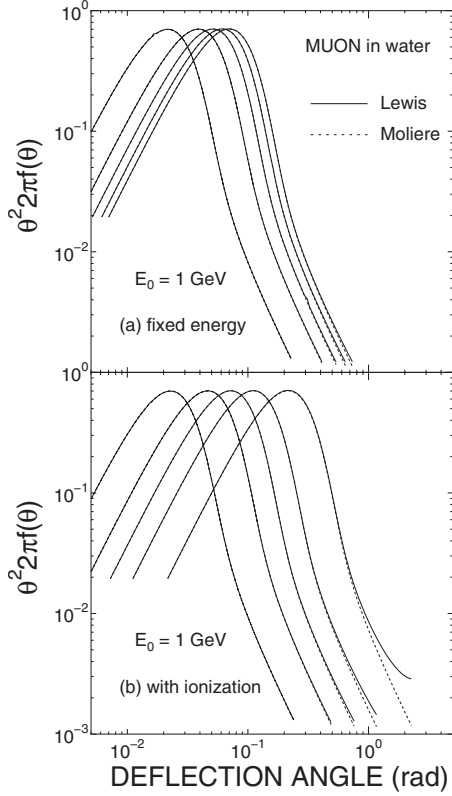


FIG. 6. Comparison of expected angular distributions multiplied by  $\theta^2$  for muons derived by the Goudsmit-Saunders and Lewis theory (solid curves) and by the Molière theory (dotted curves), assuming that the rest energy is negligible. Curves in (b) show the distributions after 39.3, 118, 197, 275, and 354 m traverses in water with ionization, from left to right, where the incident muons dissipate 10, 30, 50, 70, and 90 % of their initial energies. The curves in (a) show the distributions after the same traverses without ionization.

$$\ln \nu \approx 2 + \frac{E_0 + E}{E_0 - E} \ln \frac{E}{E_0} - \frac{m^2 c^4}{9E^2} \left( 14 + 5 \frac{E}{E_0} + 5 \frac{E^2}{E_0^2} - 12 \frac{E}{E_0} \frac{E_0 + E}{E_0 - E} \ln \frac{E_0}{E} \right). \quad (71)$$

The first two terms agree with  $\ln \nu$  under the relativistic condition, as indicated in Table I. The third term shows the next higher order term taking account of the rest energy. The exact and approximate results of the contraction factor  $\nu$  versus the fractional energy loss are compared in Fig. 7. Both agree well within an error margin of 1% up to an energy dissipation of about 70%. So we can obtain the Molière angular distribution effectively in practical uses by applying the expansion parameter  $B$  derived from Eq. (63) with the contraction factor  $\nu$  of Eq. (71) and the scale angle  $\theta_M$  derived from Eq. (9) with the Gaussian mean-square angle  $\theta_G^2$  of Eq. (70), as listed in Table I.

#### F. The scattering constants for mixed or compound material

We derive a method to obtain the Molière angular distribution of charged particles traversing through mixed or com-

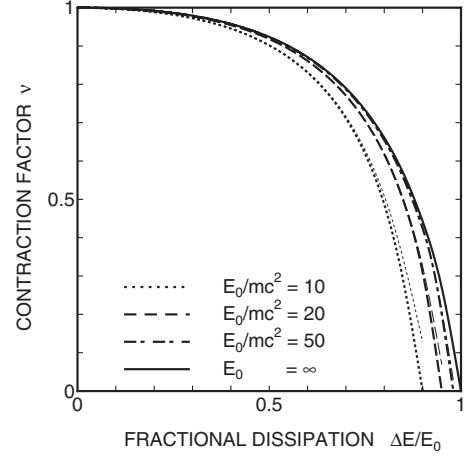


FIG. 7. Exact values of the contraction factor  $\nu$  under the condition of small Born parameter (thick curves) and their approximated values expanded by  $mc^2/E$  up to the second order (thin curves). Abscissa denotes the fraction of dissipated energy, i.e.,  $(E_0 - E)/E_0$ .

ound materials with ionization. The increment of Hankel transform of the angular distribution is expressed as

$$d\tilde{f} = -\frac{\zeta^2}{w^2} \tilde{f} \left( 1 - \frac{1}{\Omega} \ln \frac{\beta'^2 \zeta^2}{w^2} \right) z^2 dt. \quad (72)$$

Separating the terms by independent Fourier components, we have

$$-d \ln \tilde{f} = \frac{1}{X_0 w^2} \left( 1 - \frac{1}{\Omega} \ln \frac{\beta'^2}{w^2} \right) \zeta^2 z^2 dx - \frac{1}{X_0 w^2 \Omega} (\zeta^2 \ln \zeta^2) z^2 dx. \quad (73)$$

In the case of particles traversing through a mixed or compound material, the coefficients appearing in the right-hand side change discontinuously, corresponding to the atoms they encounter. So we take their stochastic means as the actual coefficient values in this case. Then we have

$$\tilde{f} = \frac{1}{2\pi} \exp \left\{ -\zeta^2 \int_0^x \Pr \left[ \frac{1}{X_0 w^2} \left( 1 - \frac{1}{\Omega} \ln \frac{\beta'^2}{w^2} \right) \right] z^2 dx + \zeta^2 \ln \zeta^2 \int_0^x \Pr \left[ \frac{1}{X_0 \Omega w^2} \right] z^2 dx \right\}, \quad (74)$$

where the stochastic mean is defined by the weighted mean value by the fraction  $p_i$  of mass:

$$\Pr[Q] \equiv \sum_i p_i Q_i. \quad (75)$$

To simplify the solution (74), we introduce the scattering constants for mixed or compound material  $\bar{\Omega}$  and  $\bar{K}$  satisfying

$$\frac{\bar{K}^2}{\bar{X}_0} \left( 1 - \frac{1}{\bar{\Omega}} \ln \frac{\bar{K}^2}{U^2} \right) = \Pr \left[ \frac{K^2}{X_0} \left( 1 - \frac{1}{\Omega} \ln \frac{K^2}{U^2} \right) \right], \quad (76)$$

$$\frac{\bar{K}^2}{\bar{X}_0\bar{\Omega}} = \Pr\left[\frac{K^2}{X_0\Omega}\right], \quad (77)$$

where  $\bar{X}_0$  denotes the radiation length for the compound material [24]

$$\bar{X}_0^{-1} = \Pr[X_0^{-1}], \quad (78)$$

and  $U$  an arbitrary unit of energy [37], so that  $\bar{\Omega}$  and  $\bar{K}$  are determined as

$$\bar{\Omega} - \ln \bar{\Omega} = \Pr\left[\frac{K^2}{X_0\Omega}\right]^{-1} \Pr\left[\frac{K^2}{X_0}\left(1 - \frac{1}{\Omega} \ln \frac{K^2}{U^2}\right)\right] + \ln\left\{\frac{\bar{X}_0}{U^2} \Pr\left[\frac{K^2}{X_0\Omega}\right]\right\}, \quad (79)$$

$$\bar{K}^2 = \bar{X}_0\bar{\Omega} \Pr\left[\frac{K^2}{X_0\Omega}\right]. \quad (80)$$

Then we have

$$\int_0^x \Pr\left[\frac{1}{X_0\Omega w^2}\right] z^2 dx = \int_0^x \frac{\bar{K}^2}{4\bar{X}_0\bar{\Omega} p^2 v^2} z^2 dx = \frac{\bar{\theta}_G^2}{4\bar{\Omega}}, \quad (81)$$

where

$$\bar{\theta}_G^2 = \frac{\bar{K}^2}{2\bar{\varepsilon}mc^2} \left\{ \frac{mc^2}{pv} - \frac{mc^2}{p_0v_0} + \frac{1}{2} \ln \frac{(E_0 - mc^2)/(E - mc^2)}{(E_0 + mc^2)/(E + mc^2)} \right\} \quad (82)$$

denotes the Gaussian mean-square deflection angle under the compound material with energy loss of a constant rare

$$\bar{\varepsilon} \equiv \bar{X}_0 \Pr[\varepsilon/X_0] \quad (83)$$

in the unit radiation length. Thus the solution (74) can be expressed as

$$\tilde{f} = \frac{1}{2\pi} \exp\left\{-\zeta^2 \int_0^x \Pr\left[\frac{1}{X_0 w^2}\left(1 - \frac{1}{\Omega} \ln \frac{\beta'^2}{w^2}\right)\right] z^2 dx + \frac{\bar{\theta}_G^2}{4\bar{\Omega}} \zeta^2 \ln \zeta^2\right\}. \quad (84)$$

So, applying the transport formula introduced in Appendix B, we have the Molière angular distributions of Eqs. (10) and (11) with the characteristic parameters  $B$  and  $\theta_M$  of

$$B - \ln B = \frac{4\bar{\Omega}}{\bar{\theta}_G^2} \int_0^x \Pr\left[\frac{1}{X_0 w^2}\left(1 - \frac{1}{\Omega} \ln \frac{\beta'^2}{w^2}\right)\right] z^2 dx + \ln \frac{\bar{\theta}_G^2}{4\bar{\Omega}}, \quad (85)$$

$$\theta_M = \bar{\theta}_G \sqrt{B/\bar{\Omega}}. \quad (86)$$

The scattering constants for the mixture  $\bar{\Omega}$  and  $\bar{K}$  together with  $\bar{\varepsilon}$  are listed in Table IV.

In the case of small Born parameter under the Molière screening model

TABLE IV. The scattering constants  $\bar{\Omega}$  and  $\bar{K}$  under the Molière screening model and the critical energies  $\bar{\varepsilon}$  for the mixture revised to be consistent with the Table of Atomic and Nuclear Properties of Materials in *The Review of Particle Physics* [24].

Material	$\bar{X}_0$ (g/cm <sup>2</sup> )	$\bar{\varepsilon}$ (MeV)	$\bar{\Omega}$	$\bar{K}$ (MeV)
Air <sup>a</sup>	36.67	86.0	15.21	19.09
SiO <sub>2</sub>	27.04	51.0	14.96	19.34
H <sub>2</sub> O	36.00	91.5	15.23	19.06
LiH	79.24	164.9	15.89	18.65
G-5 emulsion <sup>b</sup>	11.32	17.7	13.94	20.01
NaI	9.45	13.4	13.67	20.13
CsI	8.39	11.0	13.60	20.24
BGO <sup>c</sup>	7.97	10.6	13.15	20.53

<sup>a</sup>Fractional weight of 76.9% N, 21.8% O, and 1.3% Ar.

<sup>b</sup>Composed of 1.817 Ag, 1.338 Br, 0.012 I, 0.277 C, 0.053 H, 0.249 O, 0.074 N, and 0.007 S, in units of g/cm<sup>3</sup>.

<sup>c</sup>Bismuth germanate (Bi<sub>2</sub>O<sub>3</sub>)<sub>2</sub>(GeO<sub>2</sub>)<sub>3</sub>.

$$\alpha \equiv zZ/(137\beta) \ll 1, \quad (87)$$

it holds  $\beta' \approx \beta$ , so that Eq. (85) to give the expansion parameter  $B$  becomes

$$B - \ln B \approx \frac{4\bar{\Omega}}{\bar{\theta}_G^2} \left( \frac{\bar{\theta}_G^2}{4} - \frac{\bar{\theta}_G^2}{4\bar{\Omega}} \ln \frac{\beta^2 \bar{\theta}_G^2}{4\bar{v}z^2 t} \right) + \ln \frac{\bar{\theta}_G^2}{4\bar{\Omega}} = \bar{\Omega} - \ln \bar{\Omega} + \ln \frac{\bar{v}z^2 t}{\beta^2}, \quad (88)$$

where

$$\ln \bar{v} = \ln \frac{\bar{\theta}_G^2 p^2 v^2}{\bar{K}^2 z^2 t} - \frac{2z^2 \bar{\varepsilon}}{\bar{\theta}_G^2} \int_0^t \frac{\bar{\theta}_G^2}{pv} dt. \quad (89)$$

So we can get the Molière angular distributions for mixed or compound materials simply from  $B$  and  $\theta_M$  of Eqs. (88) and (86), just as from Eqs. (63) and (9) like for the pure materials having the scattering constants  $\bar{\Omega}$  and  $\bar{K}$ .

The characteristic parameters  $B$  and  $\theta_M$  exactly described by Eqs. (85) and (86) for compound materials are compared with those conventionally described by Eqs. (88) and (86) approximating  $\beta'$  by  $\beta$ , for air and nuclear emulsion in Figs. 8 and 9. We cannot find any visible differences of more than 0.1% between them within a traversed thickness up to an energy dissipation of about 90% [38].

## V. CROSS-SECTION DIVIDING MODEL TO INTERPRET THE MOLIÈRE EXPANSION OF ANGULAR DISTRIBUTION

We investigate a physical mechanism to provide the Molière series expansion and to interpret the change in the shape of the Molière angular distribution as the traversed thickness increases. We discuss the problem in this section for singly charged relativistic particles as in Eq. (1). Then the

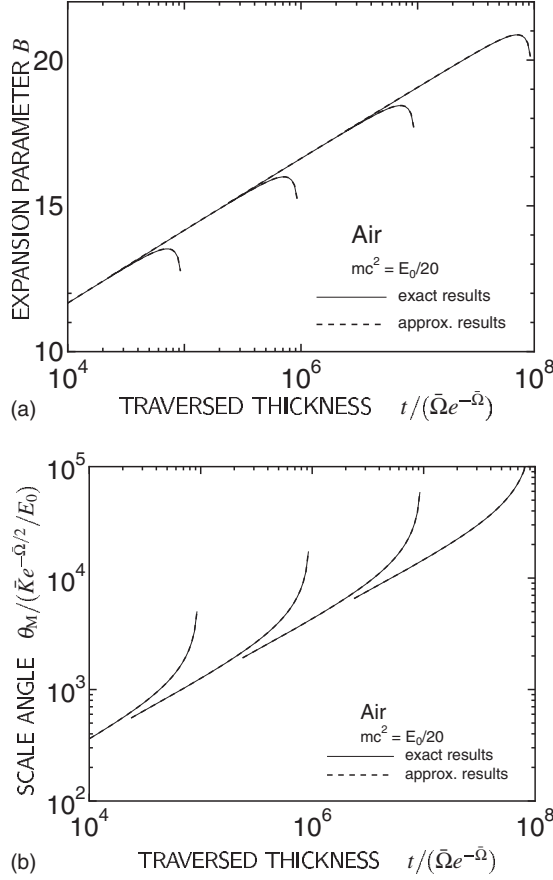


FIG. 8. Comparison between the exact  $B$  (a) and  $\theta_M$  (b) for a compound material, air, and the approximated results derived with  $\beta'$  replaced by  $\beta$ . The four branches of the curve correspond to the incident energies  $E_0$  of  $10^5$ ,  $10^6$ ,  $10^7$ , and  $10^8$  from left to right, in units of  $\bar{\Omega}e^{-\bar{\Omega}}\varepsilon$ , where the rest energies are all assumed to be  $E_0/20$ .

single-scattering formula (47) can be written as

$$\frac{N}{A}\sigma(\theta)2\pi\theta d\theta dx = \frac{1}{\pi\Omega} \frac{K^2}{E^2} \theta^{-4} 2\pi\theta d\theta dt \quad \text{with } \theta > \sqrt{e}\chi_a \quad (90)$$

by using our scattering constants  $\Omega$  and  $K$ , where the screening angle (48) is described as

$$\sqrt{e}\chi_a = (K/E)e^{-\Omega/2+1-C}. \quad (91)$$

Following the diffusion equations (35) and (37) in Sec. IV, Hankel transform of the Molière angular distribution for these particles under the azimuthally symmetric condition can be evaluated by using formula (40):

$$\begin{aligned} \tilde{f} &= \frac{1}{2\pi} \exp \left\{ \int_0^t \frac{2dt}{\Omega} \frac{K^2}{E^2} \int_{\sqrt{e}\chi_a}^{\infty} [J_0(\zeta\theta) - 1] \theta^{-3} d\theta \right\} \\ &= \frac{1}{2\pi} \exp \left\{ \int_0^t \left[ \frac{1}{\Omega} \frac{K^2 \zeta^2}{4E^2} \ln \frac{(\sqrt{e}\chi_a)^2 \zeta^2}{4e^{2-2C}} + O(\zeta^4) \right] dt \right\}. \end{aligned} \quad (92)$$

As  $\sqrt{e}\chi_a$  of Eq. (91) is proportional to  $E^{-1}$  and it holds that

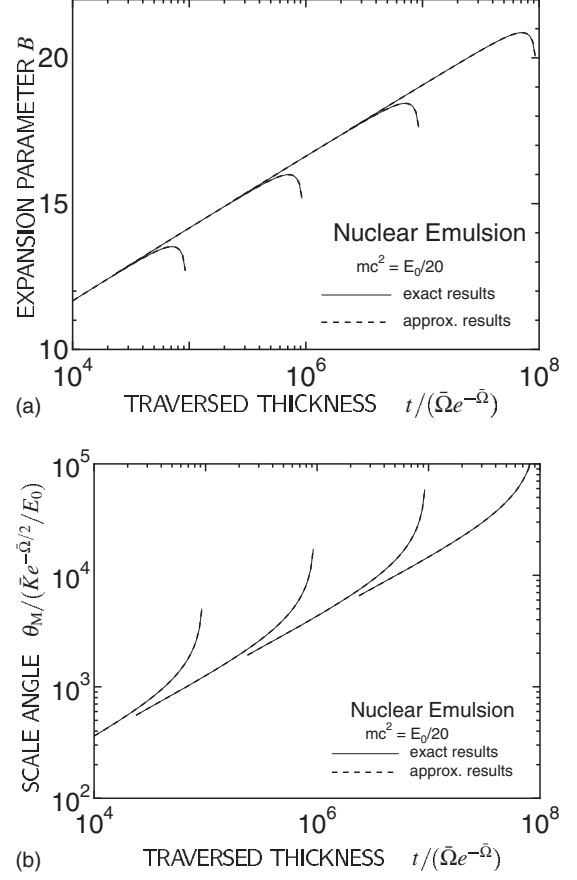


FIG. 9. Comparison between the exact  $B$  (a) and  $\theta_M$  (b) for a compound material, nuclear emulsion, and the approximated results derived with  $\beta'$  replaced by  $\beta$ . The four branches of the curve correspond to the incident energies  $E_0$  of  $10^5$ ,  $10^6$ ,  $10^7$ , and  $10^8$  from left to right, in units of  $\bar{\Omega}e^{-\bar{\Omega}}\varepsilon$ , where the rest energies are all assumed to be  $E_0/20$ .

$$\int_0^t \frac{K^2}{E^2} dt = \frac{K^2 t}{E_0 E} \quad \text{and} \quad \int_0^t \frac{K^2}{E^2} \ln \frac{K^2}{E^2} dt = \frac{K^2 t}{E_0 E} \ln \frac{K^2}{\nu E_0 E} \quad (93)$$

with  $\nu$  of Eq. (17) under the ionization process of a constant dissipating rate, we have

$$\tilde{f} = \frac{1}{2\pi} \exp \left\{ \frac{1}{\Omega} \frac{K^2 \zeta^2 t}{4E_0 E} \ln \frac{(\sqrt{e}\hat{\chi}_a)^2 \zeta^2}{4e^{2-2C}} + O(\zeta^4) \right\}, \quad (94)$$

where  $\sqrt{e}\hat{\chi}_a$  denotes the effective screening angle under the ionization process

$$\sqrt{e}\hat{\chi}_a = (K/\sqrt{\nu E_0 E})e^{-\Omega/2+1-C}. \quad (95)$$

In order to investigate the qualitative properties of the Molière scattering process, we divide the cross section  $\sigma$  into the moderate scattering  $\sigma_M$  and the large-angle scattering  $\sigma_L$  at a certain fixed separation angle  $\chi'_B$  determined later, as illustrated in Fig. 10:

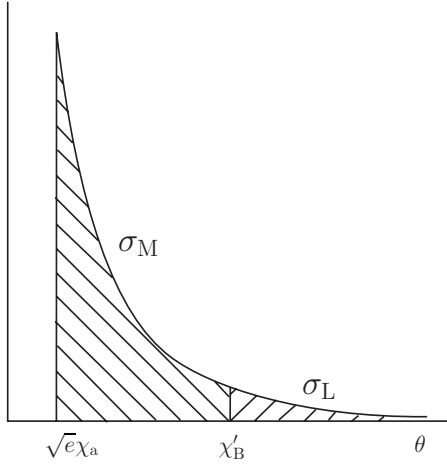


FIG. 10. Division of the single-scattering cross section  $\sigma$  at  $\chi_B'$  into the moderate scattering  $\sigma_M$  and the large-angle scattering  $\sigma_L$ .

$$\sigma(\theta) = \sigma_M(\theta) + \sigma_L(\theta). \quad (96)$$

Then the exponent of Eq. (94) can be expressed by the sum of two individual contributions from the cross sections  $\sigma_M$  and  $\sigma_L$ :

$$\begin{aligned} & \int_0^x 2\pi \frac{N}{A} dx \int_0^\infty [J_0(\zeta\theta) - 1] \sigma_M(\theta) \theta d\theta \\ &= -\frac{1}{\Omega} \frac{K^2 \zeta^2 t}{4E_0E} \ln \frac{\chi_B'^2}{(\sqrt{e}\chi_a)^2} + O(\zeta^4), \end{aligned} \quad (97)$$

$$\begin{aligned} & \int_0^x 2\pi \frac{N}{A} dx \int_0^\infty [J_0(\zeta\theta) - 1] \sigma_L(\theta) \theta d\theta \\ &= \frac{1}{\Omega} \frac{K^2 \zeta^2 t}{4E_0E} \ln \frac{\chi_B'^2 \zeta^2}{4e^{2-2C}} + O(\zeta^4). \end{aligned} \quad (98)$$

Neglecting the terms of  $O(\zeta^4)$  and introducing the expansion parameter  $B'$  and the scale angle  $\theta_M'$  corresponding to the separation angle  $\chi_B'$ ,

$$B' \equiv \ln \frac{\chi_B'^2}{(\sqrt{e}\chi_a)^2} \quad \text{and} \quad \theta_M'^2 \equiv \frac{B'}{\Omega} \theta_G^2 \quad (99)$$

with the Gaussian mean-square angle  $\theta_G^2$  of Eq. (16), we have

$$\begin{aligned} \tilde{f} &= \frac{1}{2\pi} \exp \left\{ -\frac{\theta_M'^2 \zeta^2}{4} \left( 1 - \frac{1}{B'} \left[ \ln \frac{\theta_M'^2 \zeta^2}{4} - \ln \tau \right] \right) \right\} \\ & \quad \text{with } \tau \equiv (\theta_M'/\chi_B')^2 e^{2-2C}. \end{aligned} \quad (100)$$

$\theta_M'^2$  denotes the mean square angle of the central Gaussian distribution produced by the moderate scattering  $\sigma_M$ . A thorough expansion of Eq. (100) gives the angular distribution in double power series of  $B'^{-1}$  and  $\ln \tau$ , similar to Eq. (A3) in Appendix A [39]:

$$\begin{aligned} 2\pi f(\vartheta) &= f^{(0)}(\vartheta) + \frac{1}{B'} \{ f^{(1)}(\vartheta) + f_1^{(1)}(\vartheta) \ln \tau \} + \frac{1}{B'^2} \{ f^{(2)}(\vartheta) \\ & \quad + f_1^{(2)}(\vartheta) \ln \tau + f_2^{(2)}(\vartheta) (\ln \tau)^2 \} + \dots, \end{aligned} \quad (101)$$

where  $\vartheta$  denotes the deflection angle in the unit of the scale angle  $\vartheta \equiv \theta/\theta_M'$ .

Up to now,  $\chi_B'$  or  $B'$  has been left as an arbitrary constant, so we can take  $\chi_B'$  to satisfy

$$\chi_B' = \theta_M' e^{1-C} \quad (102)$$

to make  $\tau=1$ , so that  $\ln \tau$  in Eq. (100) vanishes. Then Eq. (102) substituted with Eqs. (95) and (99) gives the exact expansion parameter  $B$  of Eq. (18), and hence gives the exact scale angle  $\theta_M$  of Eq. (9) while making series (101) the simple power series (10) of Molière.

This means the shape of the central Gaussian distribution  $f^{(0)}(\vartheta)$  is not affected by the large-angle scattering  $\sigma_L$  when we divide the single-scattering cross section  $\sigma$  at  $\chi_B'$  to satisfy Eq. (102). On the contrary, bad selections of  $\chi_B'$  different from  $\chi_B$  change the mean-square angle  $\theta_M'^2$  of the central Gaussian distribution by a factor of magnitude  $1+B'^{-1} \ln \tau$  as understood in Eq. (100), thus producing supplementary terms with  $\ln \tau$  appearing in the double power series (101).

When we divide the single-scattering cross section at  $\chi_B'$ , Eq. (100) can be expanded as

$$\tilde{f} = \frac{1}{2\pi} \exp \left\{ -\frac{\theta_M'^2 \zeta^2}{4} \right\} \sum_{k=0}^{\infty} \frac{1}{k!} \left\{ \frac{1}{B} \frac{\theta_M'^2 \zeta^2}{4} \ln \frac{\theta_M'^2 \zeta^2}{4} \right\}^k. \quad (103)$$

The factor  $B^{-1}(\theta_M'^2 \zeta^2/4) \ln(\theta_M'^2 \zeta^2/4)$  in the summation denotes the integration (98). The initial term ( $k=0$ ) of the expansion (103), so that  $f^{(0)}$  of the Molière series (10), means the Gaussian distribution produced by a lot of moderate scatterings  $\sigma_M$  within the thickness  $t$  [40]. As integrals in the diffusion equation (35) and its Fourier transform (37) tell us, each multiplication of the Fourier component  $B^{-1}(\theta_M'^2 \zeta^2/4) \ln(\theta_M'^2 \zeta^2/4)$  broadens any objective angular distribution by one more large-angle scattering  $\sigma_L$  and makes the source objective distribution vanish, depending on the probability  $p$  of undergoing the large-angle scattering within the traversed thickness  $t$ ;

$$p \equiv \frac{N}{A} \int_0^x dx \int_0^\infty \sigma_L(\theta) 2\pi \theta d\theta = \frac{\nu t}{\Omega} e^{-B+\Omega-2+2C} = \frac{1}{B} e^{2C-2}. \quad (104)$$

So we find the  $k$ th term of Eq. (103) or the  $k$ th term  $B^{-k} f^{(k)}$  of the Molière series (10),

$$B^{-k} \tilde{f}^{(k)} \equiv \frac{1}{2\pi} \frac{1}{k!} \left\{ \frac{1}{B} \frac{\theta_M'^2 \zeta^2}{4} \ln \frac{\theta_M'^2 \zeta^2}{4} \right\}^k \exp \left\{ -\frac{\theta_M'^2 \zeta^2}{4} \right\}, \quad (105)$$

means the correction term of the preceding series due to the  $k$  times successive large-angle scattering  $\sigma_L$ , by its probability of  $(B^{-1} e^{2C-2})^k/k!$  within the thickness  $t$  ( $k>0$ ). Note that the expansion parameter  $B$  acts as the probability parameter by Eq. (104), so that the Molière series (10) usually shows

rapid convergence due to the small probability of large-angle scattering as  $B$  usually takes much greater value (nearly equal to  $\Omega$  of about 10, as indicated in Table III) than  $e^{2C-2}=0.429\dots$ .

The asymptotic feature of the Molière distribution at a sufficiently large angle is expressed as  $2B^{-1}\vartheta^{-3}d\vartheta$  as derived from the asymptotic value of the second term  $B^{-1}f^{(1)}(\vartheta)\vartheta d\vartheta$  of the Molière expansion (10). The term also agrees with the integration of the single-scattering distribution (90) through the whole thickness  $t$  under the ionization process

$$\frac{2\pi\theta d\theta}{\pi\Omega}\theta^{-4}\int_0^t\frac{K^2}{E'^2}dt'=\frac{2}{\Omega}\left(\frac{\theta}{\theta_G}\right)^{-3}d\left(\frac{\theta}{\theta_G}\right)=\frac{2}{B}\left(\frac{\theta}{\theta_M}\right)^{-3}d\left(\frac{\theta}{\theta_M}\right)=2B^{-1}\vartheta^{-3}d\vartheta, \quad (106)$$

as under the fixed-energy process discussed by Bethe [13].

The mean free path  $\langle t \rangle_{\text{MFP}}$  of the single scattering (90) under radiation length becomes

$$\langle t \rangle_{\text{MFP}}=1\left/\int_{\sqrt{e}\hat{\chi}_a}^{\infty}\frac{2K^2}{\Omega E^2}\theta^{-3}d\theta\right.=\Omega e^{-\Omega}e^{2-2C}, \quad (107)$$

irrespective of the energies of the penetrating particle. In addition, the number of single scatterings larger than any fixed angle  $\chi$  within the thickness of  $t$  becomes

$$\int_0^t\frac{2K^2dt}{\Omega E^2}\int_{\chi}^{\infty}\theta^{-3}d\theta=\frac{K^2t}{\Omega E_0E\chi^2}\equiv\frac{\chi_c^2}{\chi^2}, \quad (108)$$

where  $\chi_c$ , defined as

$$\chi_c=\theta_G/\sqrt{\Omega} \quad (109)$$

with the Gaussian root-mean-square angle  $\theta_G$  of Eq. (16), is called the characteristic angle [12,13], larger than which we can expect exactly one scattering within the thickness  $t$ .

As Eqs. (99) and (102) show us, the separation angle  $\chi_B$  agrees with  $e^{B/2}$  times the effective screening angle  $\sqrt{e}\hat{\chi}_a$  and also agrees with  $e^{1-C}\sqrt{B}$  times the characteristic angle  $\chi_c$  of Eq. (109). So the value of  $e^B/B$  becomes

$$\frac{1}{B}e^B=e^{2-2C}\frac{\chi_c^2}{(\sqrt{e}\hat{\chi}_a)^2}, \quad (110)$$

giving  $e^{2-2C}$  times the number of effective scatterings larger than  $\sqrt{e}\hat{\chi}_a$  within the thickness  $t$ , as Bethe showed in his Eq. (22) under the fixed-energy case [13]. As  $e^B/B$  increases monotonously with  $B$  within its valid range of  $B > 1$ , the change of  $B$  can be interpreted by the change of  $e^B/B$  of Eq. (110). Under the fixed-energy process, the numerator  $e^{1-C}\chi_c$  from Eq. (109) with Eq. (6) increases proportionally to  $t^{1/2}$  with the traversed thickness, whereas the denominator  $\sqrt{e}\hat{\chi}_a$  of Eq. (91) stays constant, as indicated in Fig. 11. So we find  $e^B/B$ , and thus  $B$ , increases monotonously with the traversed thickness. On the other hand, under the ionization process, the effective screening angle  $\sqrt{e}\hat{\chi}_a$  of Eq. (95) increases proportionally to  $E^{-1/2}$  at the first stage ( $E \approx E_0$ ) but proportionally to  $E^{-1}$  at the last stage ( $E \ll E_0$ ) with energy dissipating at a constant rate, since the contraction factor  $\nu$  of Eq. (17) decreases as

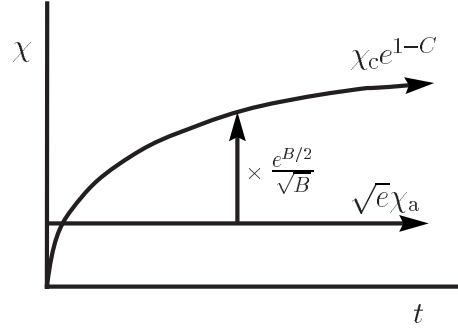


FIG. 11.  $B$  can be determined by the number of collisions  $e^{2C-2}e^B/B$  or the square of the ratio of the characteristic angle  $\chi_c$  to the screening angle  $\sqrt{e}\chi_a$  under the fixed-energy process.  $e^B/B$  is an increasing function of  $B$  within its valid range of  $B > 1$ , and the ratio increases monotonously with the increase of the traversed thickness  $t$ . So  $B$  increases monotonously with the increase of the traverse under the fixed-energy process.

$$\nu \approx \begin{cases} 1 - \frac{1}{6}\left(\ln \frac{E}{E_0}\right)^2 & (E \approx E_0), \\ e^2(E/E_0) & (E \ll E_0), \end{cases} \quad (111)$$

whereas the numerator

$$e^{1-C}\chi_c=e^{1-C}\frac{K\sqrt{t}}{\sqrt{\Omega E_0 E}}=e^{1-C}\frac{K\sqrt{E_0-E}}{\sqrt{\Omega \varepsilon E_0 E}} \quad (112)$$

from Eq. (109) with Eq. (16) increases far rapidly at the first stage but more slowly in proportion to  $E^{-1/2}$  than  $E^{-1}$  of  $\sqrt{e}\hat{\chi}_a$  at the last stage, as indicated in Fig. 12. So we find that  $e^B/B$ , and thus  $B$ , increases at the first stage of penetration, but nevertheless begins to decrease at the last stage.

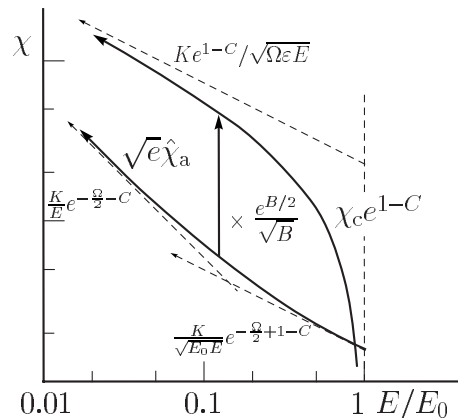


FIG. 12.  $B$  can be determined by the number of collisions  $e^{2C-2}e^B/B$  or the square of the ratio of the characteristic angle  $\chi_c$  to the effective screening angle  $\sqrt{e}\hat{\chi}_a$  under the ionization process.  $e^B/B$  is an increasing function of  $B$  within its valid range of  $B > 1$ .  $\chi_c$  increases rapidly at the first stage of traverse but increases with  $E^{-1/2}$  at the last stage with dissipation of energy. On the other hand,  $\sqrt{e}\hat{\chi}_a$  increases slowly at the first stage but increases more rapidly with  $E^{-1}$  than  $\chi_c$  at the last stage with dissipation of energy. So  $B$  increases at the first stage, nevertheless it begins to decrease at the last stage of traverse, under the ionization process.

## VI. CONCLUSION AND DISCUSSION

The Molière theory of multiple Coulomb scattering is improved to take account of ionization loss by applying our differential formulation of the theory, equivalent to the original Molière-Bethe formulation. As our diffusion equation is expressed by a simple ordinary differential equation of the first order with the traversed thickness after applying Hankel transform to the angular variable, and as all the scattering properties of traversed material are included in two scattering constants  $\Omega$  and  $K$  appearing in the coefficients, the problem has become far easier to solve even if we take ionization loss into account.

Molière angular distribution with ionization is also described in series expansion with the same universal functions  $f^{(n)}(\vartheta)$  as under the fixed-energy process for relativistic charged particles of  $\beta \approx 1$ , except with the expansion parameter  $B$  and the scale angle  $\theta_M$  corrected by the contraction factor  $\nu$  introduced under the ionization process. We found that  $B$  and  $\theta_M$ , and thus the Molière angular distribution, for these particles with energy loss of a constant rate can be expressed by the traditional results under the fixed-energy process except that thickness  $t$  and energy  $E$  are replaced by the effective ones  $\nu t$  and  $\sqrt{\nu E_0 E}$ . Using our improved angular distributions, we can take longer step-size in tracing charged particles in computer simulations without anxiety of decrease of the energy [21,41].

The distribution for arbitrary linear combination  $a\vec{\theta} + b\vec{r}/t$  between the deflection angle  $\vec{\theta}$  and the lateral displacement  $\vec{r}$  (or the chord angle  $\vec{r}/t$ ) was also derived under the ionization process. At the traversed thickness where charged particles completely dissipate their energies, only the lateral displacement  $\vec{r}$  has the Molière distribution with finite characteristic parameters  $B$  and  $\theta_M$ , while other linear combinations do not have the Molière distribution because the characteristic parameters cannot be defined at the limit.

Our differential formulation of the Molière theory is applied to charged particles of moderate energies, taking the rest energy of the particles into account. Molière angular distribution with ionization for these particles is also expressed by the traditional formula under the fixed-energy process except that  $B$  and  $\theta_M$  are corrected by  $\nu$ . The contraction factor  $\nu$  for these particles is derived through a numerical integration. We found  $\ln \nu$  for charged particles of moderate energies is well approximated merely by adding the first higher term with  $mc^2/E$  to the initial  $\ln \nu$  for relativistic particles. We have found that Goudsmit-Saunderson angular distribution with ionization is also expressed explicitly by using the same  $B$  and  $\theta_M$  derived for the Molière angular distribution. The scattering constants  $\Omega$  and  $K$ , characterizing the scattering properties of traversed material, are revised for pure materials and mixed or compound materials.

The transport mechanism of the multiple scattering process is well interpreted by dividing the single-scattering cross section  $\sigma$  into the moderate scattering  $\sigma_M$  and the large-angle scattering  $\sigma_L$  at the separation angle  $\chi_B$ , as a first approximation. The high-frequency moderate scattering generates the primary Gaussian distribution, and the low-frequency large-angle scatterings correct the Gaussian distri-

bution successively, corresponding to the number of large-angle scatterings within the thickness. The Molière series corresponds to the separation angle  $\chi_B$  of  $e^{B/2}$  times the effective screening angle  $\sqrt{e}\hat{\chi}_a$ , only when the large-angle scattering does not interfere with the width of the primary Gaussian distribution. The probability for charged particles to undergo the large-angle scattering within the thickness agrees with  $e^{2C-2}B^{-1}$ , where  $B$  denotes the expansion parameter, so we find the Molière series (10) is an expansion of the angular distribution by the probabilities of  $k$  times successive large-angle scattering.

The change of the value  $B$  with the traversed thickness is interpreted by the change of the number of scatterings larger than the effective screening angle  $\chi_c^2/(\sqrt{e}\hat{\chi}_a)^2$ . Due to more rapid increase of the effective screening angle  $\sqrt{e}\hat{\chi}_a$  than increase of the characteristic angle  $\chi_c$  with decrease of the energy, the value of  $B$  decreases at the last stage of penetration under the ionization process.

The Molière angular distribution with ionization, derived through our differential formulation of the theory, will help us design and analyze experiments relating to fast charged particles with improved accuracy. It will also be valuable for the reliable and effective tracing of charged particles in Monte Carlo simulations of single-particle transports and cascade shower processes [21,22,42–46].

## ACKNOWLEDGMENTS

The authors wish to express their deep gratitude to Dr. S. Tanaka for reading and improving their manuscript.

## APPENDIX A: MOLIÈRE ANGULAR DISTRIBUTION EXPRESSED IN A DOUBLE POWER SERIES

Another derivation of Molière angular distribution by double power series without introducing Molière's characteristic parameters  $B$  and  $\theta_M$  through his transcendental equation (7.1) [12] will be valuable, as we could not find any description in a simple power series for a certain Molière distribution [28].

The integration (5) is expanded as

$$\begin{aligned} \tilde{f} &= \frac{1}{2\pi} \exp \left\{ -\frac{\alpha^2}{4} \left( 1 - \frac{1}{\Omega} \left[ \ln \frac{\alpha^2}{4} - \ln t \right] \right) \right\} \\ &= \frac{1}{2\pi} \exp \left\{ -\frac{\alpha^2}{4} \right\} \sum_{k=0}^{\infty} \frac{1}{\Omega^k k!} \left( \frac{\alpha^2}{4} \right)^k \left( \ln \frac{\alpha^2}{4} - \ln t \right)^k, \end{aligned} \quad (\text{A1})$$

where we introduce new scale variables

$$\alpha = \theta_G \zeta \quad \text{and} \quad \phi = \theta / \theta_G. \quad (\text{A2})$$

Then, applying Hankel transforms, we get the Molière angular distribution in double power series with  $\Omega^{-1}$  and  $\ln t$ ,

$$\begin{aligned} 2\pi f(\phi) &= f^{(0)}(\phi) + \Omega^{-1} \{ f^{(1)}(\phi) + f_1^{(1)}(\phi) \ln t \} \\ &\quad + \Omega^{-2} \{ f^{(2)}(\phi) + f_1^{(2)}(\phi) \ln t + f_2^{(2)}(\phi) (\ln t)^2 \} + \dots \end{aligned} \quad (\text{A3})$$

The universal functions  $f^{(0)}$ ,  $f^{(1)}$ , and  $f^{(2)}$ , derived by Molière

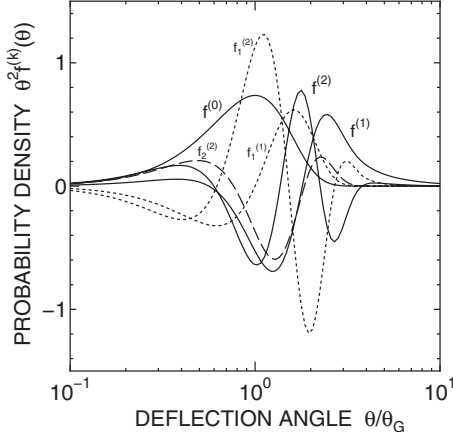


FIG. 13. Universal series functions multiplied by  $\theta^2$  appearing in the differential formulation of the Molière theory.

[11,12], and the others up to the second higher order are expressed as follows and indicated in Fig. 13:

$$f^{(0)}(\phi) = \int_0^\infty \alpha d\alpha J_0(\phi\alpha) e^{-\alpha^2/4} = 2e^{-\phi^2}, \quad (\text{A4})$$

$$\begin{aligned} f^{(1)}(\phi) &= \int_0^\infty \alpha d\alpha J_0(\phi\alpha) \frac{\alpha^2}{4} e^{-\alpha^2/4} \ln \frac{\alpha^2}{4} \\ &= 2e^{-\phi^2} (\phi^2 - 1) [E_i(\phi^2) - \ln \phi^2] - 2(1 - 2e^{-\phi^2}), \end{aligned} \quad (\text{A5})$$

$$f_1^{(1)}(\phi) = - \int_0^\infty \alpha d\alpha J_0(\phi\alpha) \frac{\alpha^2}{4} e^{-\alpha^2/4} = 2e^{-\phi^2} (\phi^2 - 1), \quad (\text{A6})$$

$$\begin{aligned} f^{(2)}(\phi) &= \frac{1}{2} \int_0^\infty \alpha d\alpha J_0(\phi\alpha) \left(\frac{\alpha^2}{4}\right)^2 e^{-\alpha^2/4} \left(\ln \frac{\alpha^2}{4}\right)^2 \\ &= e^{-\phi^2} (\phi^4 - 4\phi^2 + 2) [\psi'(3) + \psi^2(3)] \\ &\quad + 4e^{-\phi^2} \int_0^1 t^{-3} \left[ \ln \frac{t}{1-t} - \psi(3) \right] \left[ (1-t)^2 e^{\phi^2 t} - 1 \right. \\ &\quad \left. - (\phi^2 - 2)t - \frac{1}{2}(\phi^4 - 4\phi^2 + 2)t^2 \right] dt, \end{aligned} \quad (\text{A7})$$

$$\begin{aligned} f_1^{(2)}(\phi) &= - \int_0^\infty \alpha d\alpha J_0(\phi\alpha) \left(\frac{\alpha^2}{4}\right)^2 e^{-\alpha^2/4} \ln \frac{\alpha^2}{4} \\ &= 2e^{-\phi^2} (\phi^4 - 4\phi^2 + 2) [E_i(\phi^2) - \ln \phi^2] \\ &\quad + 4e^{-\phi^2} (2\phi^2 - 3) - 2(\phi^2 - 3), \end{aligned} \quad (\text{A8})$$

$$f_2^{(2)}(\phi) = \frac{1}{2} \int_0^\infty \alpha d\alpha J_0(\phi\alpha) \left(\frac{\alpha^2}{4}\right)^2 e^{-\alpha^2/4} = e^{-\phi^2} (\phi^4 - 4\phi^2 + 2). \quad (\text{A9})$$

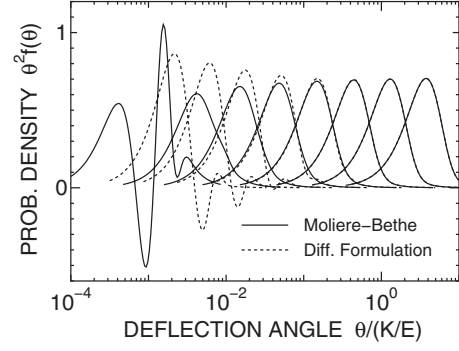


FIG. 14. Comparison of angular distributions expressed in the double power series with those expressed in the Molière simple series, at thickness  $t = e^{2k+1}\Omega e^{-\Omega}$  with  $k=0, 1, 2, \dots, 7$ , from left to right.  $\Omega e^{-\Omega}$  takes the values of the order of  $10^{-6}$ , denoting  $e^{2C-2}$  times the mean-free path of Eq. (107) of the single scattering. At very short thicknesses, the both angular distributions show oscillating features due to deficits of higher-order Fourier components.

The Molière angular distributions expressed in the double power series of Eq. (A3) are equivalent with those expressed in the simple Molière series of Eq. (10), both neglecting the next higher-order Fourier components,  $\zeta^2$  times higher or more than the constant or the logarithmic terms. We compare these two angular distributions in Fig. 14. Both agree well at moderate traverse thicknesses. When the traverse is very thin, the simple Molière series oscillates, as discussed by Bielajew *et al.* [47]. The double power series (A3) also shows bad convergence at these thicknesses due to the lack of higher-order Fourier components.

## APPENDIX B: A TRANSPORT FORMULA TO GIVE THE MOLIÈRE SIMPLE SERIES

We show a transform formula to obtain the angular distribution in the Molière simple series from the solution of the diffusion equation. Let the solution in the frequency space be of the form [48]

$$\tilde{f} = \frac{1}{2\pi} \exp\{-a\zeta^2 + b\zeta^2 \ln(c\zeta^2)\}. \quad (\text{B1})$$

If we define the expansion parameter  $B$  and the new scale variable  $u$  as

$$B - \ln B = (a/b) - \ln(c/b), \quad (\text{B2})$$

$$u = 2\zeta\sqrt{bB}, \quad (\text{B3})$$

then we get the traditional Molière form

$$\tilde{f} = \frac{1}{2\pi} \exp\left\{-\frac{u^2}{4} \left(1 - \frac{1}{B} \ln \frac{u^2}{4}\right)\right\}. \quad (\text{B4})$$

Thus, the probability density can be represented in the Molière series (10), where the Molière angle is defined as

$$\vartheta = \theta/\theta_M \quad \text{with } \theta_M = 2\sqrt{bB}. \quad (\text{B5})$$

- [1] E. J. Williams, Proc. R. Soc. London, Ser. A **169**, 531 (1939).
- [2] W. T. Scott, Rev. Mod. Phys. **35**, 231 (1963).
- [3] B. Rossi and K. Greisen, Rev. Mod. Phys. **13**, 240 (1941).
- [4] C. N. Yang, Phys. Rev. **84**, 599 (1951).
- [5] T. Nakatsuka, Phys. Rev. D **35**, 210 (1987).
- [6] L. Eyges, Phys. Rev. **74**, 1534 (1948).
- [7] G. Sandison, L. Papiez, and V. Tulovsky, Phys. Rev. E **49**, 4696 (1994).
- [8] T. Nakatsuka, Phys. Rev. D **58**, 056002 (1998).
- [9] S. A. Goudsmit and J. L. Saunderson, Phys. Rev. **57**, 24 (1940).
- [10] S. A. Goudsmit and J. L. Saunderson, Phys. Rev. **58**, 36 (1940).
- [11] G. Molière, Z. Naturforsch. A **2**, 133 (1947).
- [12] G. Molière, Z. Naturforsch. A **3**, 78 (1948).
- [13] H. A. Bethe, Phys. Rev. **89**, 1256 (1953).
- [14] H. Snyder and W. T. Scott, Phys. Rev. **76**, 220 (1949).
- [15] H. W. Lewis, Phys. Rev. **78**, 526 (1950).
- [16] G. Molière, Z. Naturforsch. A **10**, 177 (1955).
- [17] M. J. Berger and R. Wang, *Monte Carlo Transport of Electrons and Photons*, edited by T. M. Jenkins, W. R. Nelson, and A. Rindi (Plenum, New York, 1989), p. 21.
- [18] K. Kamata and J. Nishimura, Suppl. Prog. Theor. Phys. **6**, 93 (1958).
- [19] J. Nishimura, in *Handbuch der Physik, Band 46*, edited by S. Flügge (Springer, Berlin, 1967), Teil 2, p. 1.
- [20] M. Messel and D. F. Crawford, *Electron-Photon Shower Distribution Function Tables for Lead Copper and Air Absorbers* (Pergamon, Oxford, 1970).
- [21] W. R. Nelson, H. Hirayama, and D. W. O. Rogers, Stanford Linear Accelerator Center Report No. 265, 1985.
- [22] D. Heck, J. Knapp, J. N. Capdevielle, G. Shatz, and T. Thouw (unpublished).
- [23] Molière also used the differential method partially in Ref. [16] to get the distribution for a linear combination between the deflection angle and the lateral displacement under the fixed-energy condition; this fact would be another evidence to show the significance of the differential formulation.
- [24] W.-M. Yao *et al.*, J. Phys. G **33**, 1 (2006).
- [25] P. Andreo and A. Brahme, Radiat. Res. **100**, 16 (1984).
- [26] It should be noted Molière defined the differential probability as  $f(\theta, t)\theta dt$ , having integrated over the azimuthal angle.
- [27] Equation (4.10) in Kamata and Nishimura [18] or Eq. (A.3.27) in Nishimura [19].
- [28] In case of the path-length problem under the Molière theory [5], we could not find any way to express the distribution in a simple power series.
- [29] B. Rossi, *High Energy Particles* (Prentice-Hall, Englewood Cliffs, NJ, 1952).
- [30] Molière evaluated the corrective increment due to energy loss [12] in his Eqs. (6) and (13b) which agrees with our  $\ln v$ , though his term in the logarithm should be read as  $1-l/l_0$  after correction of a misprint.
- [31] We can set  $b \neq 0$ , as  $b=0$  brings  $g(\vec{\rho}, t)d\vec{\rho}$  to the angular distribution derived in Sec. II.
- [32] *Handbook of Mathematical Functions with Formulas, Graphs, and Mathematical Tables*, edited by M. Abramowitz and I. A. Stegun (Dover, New York, 1965).
- [33] W. Gröbner and N. Hofreiter, *Integraltafeln* (Springer, Wien, 1950), Vol. I.
- [34] Our ratio for  $\theta_G^2$  agrees with Molière's ratio for  $\chi_c^2$ , as  $\theta_G$  is proportional to  $\chi_c$  as indicated later in our Eq. (109).
- [35] O. I. Dovzhenko and A. A. Pomanskii, Sov. Phys. JETP **35**, 187 (1964).
- [36] Y. S. Tsai, Rev. Mod. Phys. **46**, 815 (1974).
- [37]  $U$  is introduced only to make the antilogarithm nondimensional. Resultant  $\bar{\Omega}$  does not depend on the  $U$  that we adopt.
- [38] Comparisons are also made for  $\text{H}_2\text{O}$  and  $\text{SiO}_2$  in T. Nakatsuka and J. Nishimura, *27th International Cosmic Ray Conference*, Hamburg, 2001, Conference Papers, edited by K. H. Kampert, G. Heinzelmann, and C. Spiering (Copernicus Gesellschaft, Katlenburg-Lindau, 2001), Vol. 1, p. 286.
- [39] In fact,  $\tau$  becomes  $t$  and Eq. (101) becomes Eq. (A3) when we substitute  $\Omega$  into  $B'$  under the fixed-energy condition.
- [40] Practically, the moderate scattering  $\sigma_M$  defined by the divided cross-section model with the separation angle of  $\chi_B$  gives a slight distortion to the primary Gaussian distribution due to the lack of higher order terms in Eq. (97) or the insufficient traversed thickness for  $\sigma_M$  to produce Gaussian distribution, as investigated in K. Okei and T. Nakatsuka, *28th International Cosmic Ray Conference*, Tsukuba, 2003, Conference Papers, edited by T. Kajita, Y. Asaoka, A. Kawachi, Y. Matsubara, and M. Sasaki (Universal Academy Press, Tokyo, 2003), Vol. 3, p. 1999. The corrected central distribution or other ideal division of the cross section will be needed in actual applications of this model in order to achieve very high accuracy.
- [41] A. F. Bielajew and D. W. O. Rogers, Nucl. Instrum. Methods Phys. Res. B **18**, 165 (1987).
- [42] X. Ning, L. Papiez, and G. Sandison, Phys. Rev. E **52**, 5621 (1995).
- [43] *Monte Carlo Transport of Electrons and Photons*, edited by T. W. Jenkins, W. R. Nelson, and A. Rindi (Plenum, New York, 1988).
- [44] S. M. Selzer, in Ref. [43], pp. 153–182.
- [45] J. A. Halbleib, R. P. Kensek, T. A. Mehlborn, G. D. Valdez, S. M. Selzer, and M. J. Berger (unpublished).
- [46] GEANT4 Collaboration, Nucl. Instrum. Methods Phys. Res. A **506**, 250 (2003).
- [47] A. F. Bielajew, R. Wang, and S. Duane, Nucl. Instrum. Methods Phys. Res. B **82**, 503 (1993).
- [48] Combination of coefficients  $a$  and  $c$  is not unique. We can put  $a=0$  or  $c=1$  without a loss of generality, then the other is determined uniquely.